

### 43. Study on the Propagation of Seismic Waves.

(The second paper)

#### *Amplitude of Seismic Waves with the Structure of the Earth's Crust and Mechanisms of their Origin.*<sup>1)</sup>

(Continued.)

By HIROSI KAWASUMI,

Seismological Institute.

(Received Sept. 20, 1934.)

#### Chapter V. On the Mechanism of Occurrence of the Deep-seated Ise-bay Earthquake of June 2, 1929.

This earthquake has been investigated by Mr. K. Sagisaka<sup>2)</sup>, who inferred from the "pull-push" distribution of initial motions that the earthquake was originated according to the mechanism of model *B* in which two nodal planes at right angles appear. And he called the earthquake as a fault earthquake showing also a conspicuous distribution of seismogram types<sup>3)</sup> in favour of this mechanism of earthquake occurrence. But Prof. M. Ishimoto<sup>4)</sup> on the contrary pointed out recently that the "pull-push" distribution of this earthquake was also explainable remarkably well by the mechanism of model *A* in which nodal cone surface appears. And the present writer showed that not only the direction but also the amplitude of *P*- and *S*-waves of the deep-seated Central Japan earthquake of June 2, 1931 were explainable by the same mechanism. Thus the question "which of the mechanisms of model *A* or model *B* give rise earthquakes?" arose, and the present writer examined the question with the amplitude of *P*-wave of the present earth-

1) Continuation of a paper with the same title in *Bull. Earthq. Res. Inst.*, **11** (1933), 403~453. Already published in Japanese in *Disin*, **6** (1934), 32~53; 223~246.

2) K. SAGISAKA, *Geophys. Mag.*, **3** (1930), 165~167.

3) The fact that the types of seismograms of an earthquake vary with the bearings from the hypocentre was first pointed out by late Prof. F. Omori. *Bull. Earthq. Inv. Comm.*, **1** (1907), 145~154.

4) M. ISHIMOTO, *Proc. Imp. Acad.*, **8** (1932), 36~39.

quake, while Mr. Sagisaka<sup>5)</sup> published again a paper entitled "Mechanism of motion at a hypocentre as seen from first motions of seismic transverse wave", in which he stated that no contradiction occurred though he examined the direction of *S*-wave, and he revised his former view that the earthquake was originated by normal faulting, and explained by saying that the earthquake was originated by a motion at a hypocentre such that a sphere changes its shape into an ellipsoid. He also found that no difference could be observed between the fault and nodal planes (which are perpendicular to each other according to Mr. S. I. Kunitomi's hypothesis<sup>6)</sup>) even though he examined *S*-phases of this earthquake and an after-shock of the North Idu Earthquake, and advocated that it is better to withdraw the different names as fault and nodal planes. But if we are permitted to call Prof. Matuzawa's model of doublet exciter with moment as fault earthquake, we can theoretically find evident difference in the fault and nodal planes by examining *S*-phase, though existence of such an earthquake is another problem. And we do not pursue this point further. But as Mr. Sagisaka's investigation is not based upon any theory, so that the conclusion is not decisive. And there remains the questions, "is the earthquake really inexplicable by the mechanism of model *A*?", and "how far is it explained by the mechanism of model *B*?". In the following these points were examined by a quantitative method based upon the theory of elastic waves. The method is the same as used in Chapter IV, and so this will serve as the verification of the applicability of this method.

Fortunately Mr. Sagisaka published in his paper seismograms due to this earthquake at many stations in Japan, complying the writer's request through the late Prof. K. Suyehiro, the former director of the Earthquake Research Institute, to Dr. T. Okada, the director of the Central Meteorological Observatory. And the above points could be examined by virtue of this material. The writer wishes to take this opportunity of expressing his sincere thanks to late Prof. Suyehiro, Dr. Okada and Mr. Sagisaka.

As to the position of hypocentre of this earthquake Mr. Sagisaka gave in his first paper

$$\varphi = 34^{\circ}4N, \quad \lambda = 136^{\circ}6E, \quad \text{and the depth } h = 360 \text{ km.},$$

while in his second paper we find

5) K. SAGISAKA, *Kensin Zihô*, (1932), 15~42.

6) S. I. KUNITOMI, *Geophys. Mag.*, 2 (1929), 65~89.

$$\varphi = 34^{\circ}16' N, \quad \lambda = 137^{\circ}14' E, \quad h = \text{ca. } 300 \text{ km.}$$

But such inaccuracy must have been inevitable from the observational accuracy at that time. And the writer determined the position of hypocentre so as to adapt the distribution of initial motions of  $P$ -wave. It will be of some interest to know that the hypocentre is determined by such method with a tolerable accuracy.

First the observed amplitudes of this earthquake are tabulated in Table XII. The values of  $P$ -wave are wholly extracted from Mr. Sagisaka's paper and those of  $S$ -wave were measured by the present writer from the enlarged photographic reproductions of the seismograms in Mr. Sagisaka's paper. We must correct these values for initial conditions of seismographs, but as the seismograms available were hand-written copies the correction was not executed. So the second throws ( $P_{II}'$  and  $S_{II}'$ ) were also tabulated for comparison. Moreover the magnifications of the respective seismographs were not given in the above paper, the values in the table may also be inaccurate in this sense, therefore the ratios of amplitudes of  $P$ - and  $S$ -waves are derived from the reproduced seismograms.

**1.** *Initial Motion of  $P$ -wave and the Mechanisms of Occurrence of Model A and Model B.*

Horizontal component of the observed initial motion of  $P$ -wave in the above table are written in Fig. 11 and Fig. 12. Let us first examine the mechanism of model A suggested by Prof. Ishimoto. First the depth of hypocentre was assumed to be about 328 km. for which the writer already calculated<sup>7)</sup> time distance curves and constant of seismic ray  $K$ . And the vertical angle of the nodal cone was assumed to be  $55^{\circ}$  as obtained in chapter IV from the Central Japan earthquake of June 2, 1931. Then adjusting the nodal line so as to pass through Miyazaki, Unzendake and the vicinity of Matumoto, the epicentre turned out at  $\varphi = 34^{\circ} 18' N$ ,  $\lambda = 136^{\circ} 33' E$ , and this is just the same position of Mr. Sagisaka's first epicentre. The axis of nodal cone inclines by about  $i = 25^{\circ}$  in the azimuth of  $N 70^{\circ} W$ , and the resulting loci (diagram is omitted) of equal amplitudes of calculated horizontal component are not in harmony with the distribution of observed amplitudes which is nearly symmetrical on both sides a line trending  $N 80^{\circ} W$  which seems to pass through the epicentre, moreover the positions of maximum amplitude on east and west sides of epicentre seem a little farther away from the

7) H. KAWASUMI, *Bull. Earthq. Res. Inst.*, 10 (1932), 94-129.

Table XII. Observed amplitude of *P*- and *S*-waves due to the Ise-bay earthquake, June 2, 1929.

Station	<i>P</i>			<i>P<sub>H</sub></i>	<i>S</i>			<i>S<sub>H</sub></i>	<i>P<sub>H</sub>'</i>	<i>S<sub>H</sub>'</i>	$\frac{P_H}{S_H}$	$\frac{P_H'}{S_H'}$
	<i>N</i>	<i>E</i>	<i>U</i>		<i>N</i>	<i>E</i>	<i>U</i>					
Tu	+160	-235		284	+ 636	-1705		1820	680	3884	0.11	0.18
Sionomisaki	-123	-130	+450	179		- 614			(381E)	(983E)	(E) 0.20	(E) 0.39
Sumoto	- 55	-200	+430		+199	+ 199		281	545	622	0.92	0.88
Yagi	+ 33	-300		302								
Nagoya	+136	+ 7		136	-273	- 852		895	269	1796	0.12	0.15
Gihu	+ 74	- 24		77								
Kyôto	+ 96	-157	+243	183	-193	- 295		353	365	788	0.53	0.46
Hikone	+215	- 33	+358	218								
Wakayama	+ 0	-148		148								
Numadu	- 31	- 82	-284	88	+551	- 563		788	306	1313	0.14	0.24
Takayama					+ 6	- 230		237				
Tokusima	+ 6	- 20		420								
Matumoto												
Toyooka	+128	-106		166	+222	+ 199		293	382	770	0.65	0.50
Mera	- 20	- 38	-138	43	+381	- 284		478			0.09	(0.26)
Hatizyôzima	+120	-114	-220	165	-392	- 364		535	390	797	0.30	0.49
Okayama	+100	-296		313								
Niihama	- 5	-216		216								
Yokohama	- 25	- 32	-390	41	+625	- 341		711				
Oiwake		+ 34		34								
Muroto	- 40	-156		161	+136	+ 224		262				
Kumagaya	- 60	- 12	- 95	61	+338	- 206		396				
Tôkyô	- 20	- 18	-150	27	+511	- 597		786				
Husiki	+ 53	- 10		54		-1150		1150				
Nagano	- 30	+ 31		43		-1040			(68 W)	(1330 E)	(E) 0.04	(E) 0.05
Mito		-150		150								
Tukubasan	- 75	- 79	- 10	109								
Kôti	- 25	-242		243	+341	+1522		1560	361	2879	0.17	0.13
Yamagata	- 97	- 53		111	+767	- 967		1240			0.09	
Tadotu	- 5	- 25		25								
Kakioka	- 6	- 6		8								

(to be continued.)

Table XII. (continued.)

Station	P			$P_{II}$	S			$S_{II}$	$P_{II}'$	$S_{II}'$	$\frac{P_{II}}{S_{II}}$	$\frac{P_{II}'}{S_{II}'}$
	N	E	U		N	E	U					
Tyôsi	- 38	- 70	- 52	79								
Takata	- 47	- 26	- 85	54	+220	-400		457			0.12	
Utunomiya	- 1	- 2		2								
Matuyama	- 5	-130		130								
Hirosima	- 6	- 94		94								
Hamada	+ 15	- 48	+ 53	50	+ 32	+381	+89	382			0.13	
Hukusima	- 56	-104		118								
Onahama	-100	- 26		103								
Ooita	- 52	- 44	+ 55	68								
Sendai	- 39	- 30	- 38	49	+335	-205		393			0.12	
Isinomaki	- 3	- 25		25								
Miyazaki	+ 4	- 10		10	+209	+962		988			0.01	
Simonoseki						+101						
Hukuoka					+258	+850		1177				
Kumamoto	+ 6	- 16		17								
Unzendake	+ 3	- 8		8								
Nagasaki	+ 10	20	- 19	23	-216	+239		322			0.07	
Akita	- 81	- 90	-540	121	+182	-125		221			0.55	
Morioka	- 21	- 8		22								
Miyako	- 28			28								
Aomori	- 10	- 16		19								
Taikyû		+ 8		8								
Titizima				(3)	-125	+125		177	(3)	306	0.02	0.01
Hakodate	- 10	+ 10		14								
Keizyô	- 7	- 13		15								
Zinsen	- 16	+ 44		47	+ 85	- 45		97	111	178	0.47	0.62
Sapporo												
Kusiro	- 8	- 4		9								
Taihoku	+ 11	+ 22	- 36	25	- 58	- 63		85	47	165	0.39	0.28
Isigakizima	+ 26	+ 14	- 47	30	-102	- 91		137	65	241	0.21	0.27
Kôhu	-100	- 63		118								
Kanazawa	+ 23	- 3		23	-1136	-682		1477	158	2918	0.05	0.05
Hakui	+140	75		159		-825		825			0.19	

epicentre than observed actually. So we can see the hypocentral depth assumed above was too deep. Therefore the depth 303 km. is assumed and the same loci of equal amplitude are drawn on a map which is indicated in Fig. 11, in which the previous defects are improved. Position of epicentre came out this time at

$$\varphi = 34^{\circ}16' \text{ N}, \quad \lambda = 136^{\circ}47' \text{ E.}$$

As the method of calculation of the loci is just the same as in Chapter IV, so only the necessary values for the calculation and the results are tabulated in Tables XIII and XIV.

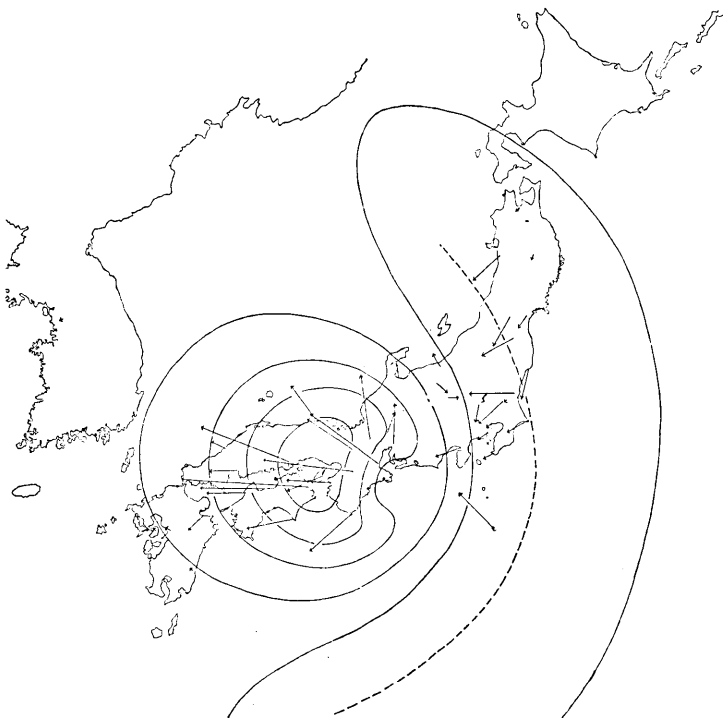


Fig. 11. Distribution of initial motion  $P$  (arrow) due to the deep-seated Ise-bay earthquake of June, 2, 1929, and isoamplitude line calculated for the mechanism of model  $A$ .

As we see from Fig 11, the "push" that is compression is entirely enclosed by a nodal line, and amplitude distribution is fairly well explained by the loci of equal amplitude, except those at Numadu and Kôhu. And this will be sufficient to support Prof. Ishimoto's opinion.

Table XIII. Necessary values of the calculation of amplitudes for earthquake with hypocentral depth of ca. 300 km.

Epicentral distance	0°	0° 34'	1° 08'	2° 14'	3° 18'	4° 20'	5° 22'	6° 23'	7° 23'	8° 23'	9° 23'	10° 23'
$u$	0	—	25° 25'	45° 05'	68° 53'	68° 43'	76° 09'	84° 48'	87° 00'	93° 00'	95° 10'	98° 33'
$e_{50}$	90°	79° 1	69° 1	54° 0	44° 7	40° 9	36° 3	34° 7	34° 0	34° 0	34° 2	34° 8
$e_{20}$	90°	81° 1	73° 1	61° 4	54° 7	53° 0	49° 0	48° 0	47° 6	47° 6	47° 7	48° 1
$e_0$	90	82° 8	76° 4	67° 1	61° 9	59° 2	57° 7	57° 0	56° 7	56° 7	56° 8	57° 1
$(\mathcal{R}'/\mathcal{R})_{50}$	1.143	—	1.124	1.107	1.052	1.034	1.000	0.990	0.984	0.984	0.986	0.991
$(\mathcal{R}'/\mathcal{R})_{20}$	1.143	—	1.130	1.112	1.094	1.088	1.073	1.070	1.069	1.069	1.070	1.071
$(u/\mathcal{R})_0$	0	—	0.54	0.88	1.06	1.15	1.20	1.22	1.23	1.23	1.22	1.21
$t_P$	40.5	—	43.6	51.6	62.0	73.6	85.6	98.0	110.3	122.6	135.0	147.2
$\frac{1}{t_P} \Pi \left( \frac{\mathcal{R}'}{\mathcal{R}} \right) \left( \frac{u}{\mathcal{R}} \right)_0$	0	—	0.01573	0.02099	0.01967	0.01578	0.01498	0.01319	0.01168	0.01051	0.00953	0.00873
$(\mathcal{R}'/\mathcal{R})_{50}$	1.143	1.140	1.114	1.080	1.060	1.032	0.992	0.976	0.970	0.970	0.972	0.976
$(\mathcal{R}'/\mathcal{R})_{20}$	1.143	1.111	1.110	1.107	1.081	1.078	1.070	1.067	1.066	1.065	1.067	1.067
$(C'/C)_{50}$	1.143	1.141	1.136	1.109	1.072	1.053	1.023	1.012	1.009	1.009	0.010	1.012
$(C'/C)_{20}$	1.143	1.142	1.140	1.124	1.110	1.105	1.090	1.088	1.085	1.085	1.010	1.012
$(u/\mathcal{R})_0$	2	-1.969	-1.905	-1.768	-1.722	-1.749	-1.820	-1.900	-1.962	-1.962	-1.960	-1.890
$(w/\mathcal{R})_0$	0	0.300	0.534	0.845	0.968	1.007	1.006	0.983	0.973	0.973	0.977	0.986
$\frac{1}{t_P} \Pi \left( \frac{\mathcal{R}'}{\mathcal{R}} \right) \left( \frac{u}{\mathcal{R}} \right)_0$	0.06474	0.05981	0.05406	0.04097	0.03182	0.02644	0.02257	0.02019	0.01840	0.01647	0.01506	0.01337
$\frac{1}{t_P} \Pi \left( \frac{\mathcal{R}'}{\mathcal{R}} \right) \left( \frac{w}{\mathcal{R}} \right)_0$	0	0.00912	0.01514	0.01957	0.01789	0.01522	0.01248	0.01045	0.00912	0.00816	0.00750	0.00698
$\frac{1}{t_P} \Pi \left( \frac{C'}{C} \right) \cdot 2$	0.06474	0.06419	0.05940	0.04831	0.03839	0.03162	0.02605	0.02247	0.01985	0.01777	0.01511	0.01391

But we must examine similarly by the mechanism of model *B* before concluding.

Table XIV. Calculated amplitude of horizontal component of *P*-wave on the earth's surface due to mechanism of model *A* for the Ise-bay earthquake.

$$\sigma_{III} = \frac{1}{t} \Pi \left( \frac{\mathcal{M}'}{\mathcal{M}} \right) \cdot \left( \frac{u}{u_0} \right) P_2(\cos \theta) \times 10^5.$$

$\theta$ $\Phi$	0°	1° 8'	2° 14'	3° 18'	4° 20'	5° 22'	6° 23'	7° 23'	8° 23'	9° 23'	10° 23'
0°	0	1573	1723	1052	496	133	- 77	-199	-305	-311	-332
15°	0	1542	1667	0991	0443	97	-106	-222	-322	-325	-341
30°	0	1458	1494	818	302	- 13	-191	-285	-368	-362	-370
45°	0	1328	1232	561	93	-174	-310	-374	-427	-419	-403
60°	0	1162	909	256	-149	-349	-438	-467	-483	-453	-412
75°	0	982	567	- 51	-390	-514	-554	-542	-520	-476	-435
90°	0	794	237	-336	-594	-644	-628	-580	-522	-467	-412
105°	0	615	- 52	-568	-745	-721	-658	-578	-488	-424	-359
120°	0	459	-294	-740	-839	-749	-645	-537	-420	-355	-281
135°	0	337	-472	-852	-872	-737	-601	-474	-336	-271	-194
150°	0	244	592	-913	-877	-706	-549	-409	-256	-192	-113
165°	0	187	-661	-942	-872	-677	-504	-357	-200	-136	-507
180°	0	168	-680	-950	-868	-664	-489	-339	-179	-116	- 37

As was already stated there are two types in the mechanism of model *B*, the Prof. Matuzawa's type and that of Prof. Hasegawa, but the space distribution of amplitude of *P*-wave is identical and the difference is seen in the space distribution of *S*-wave. But putting off the discussion of *S*-wave to the next article *P*-wave alone is discussed here.

From the equation (27) or (30) of Chapter II,

$$\left. \begin{aligned} u_1 &= A \frac{d}{dr} \left\{ \frac{H_{2+\frac{1}{2}}^{(2)}(hr)}{\sqrt{r}} \right\} \sin^2 \theta \sin(2\varphi + \varepsilon) e^{i\pi t} \\ &\approx -\sqrt{\frac{2h}{\pi}} A \frac{e^{i(\pi t - hr)}}{r} \sin^2 \theta \sin(2\varphi + \varepsilon), \\ v_1 &= A \frac{H_{2+\frac{1}{2}}^{(2)}(hr)}{r^{\frac{3}{2}}} 2 \sin \theta \cos \theta \sin(2\varphi + \varepsilon) e^{i\pi t} \approx O\left(\frac{1}{r^2}\right), \end{aligned} \right\} \dots (82)$$

$$w_2 = A \frac{H_{2\frac{1}{2}}^{(2)}(hr)}{r^{\frac{3}{2}}} 2 \sin \theta \cos (2\varphi + \varepsilon) e^{i\omega t} \approx O\left(\frac{1}{r^2}\right), \quad \left. \vphantom{w_2} \right\}$$

where  $u_1$ ,  $v_1$  and  $w_1$  are displacement of  $P$ -wave due to mechanism of model  $B$  in the direction of  $r$ ,  $\theta$  and  $\varphi$  respectively. At large distance from the origin we have only to discuss  $u_1$ . The nodal surfaces of  $P$ -wave is therefore  $2\varphi + \varepsilon = 0$  and  $\pi$ , and in the vicinity of hypocentre they are two planes intersecting each other at right angles. The line of intersections of the nodal planes is  $\theta = 0$  and is nearly horizontal in this earthquake. As the hypocentral depth of this earthquake is not known sufficiently we cannot determine the inclination of this line. So here it is assumed to be horizontal, and hypocentral depth is assumed as before to be 303 km. Transforming the coordinate axis the seismic vertical, that is the vertical line through hypocentre, is now taken as the polar axis, and the angle subtended by this polar axis and a seismic ray is denoted by  $i$ , and the azimuthal angle is represented by  $\Phi$ . Then

$$\begin{aligned} \sin^2 \theta \sin (2\varphi + \varepsilon) &= \sin^2 \theta \sin 2\varphi \cos \varepsilon + \sin^2 \theta \cos 2\varphi \sin \varepsilon \\ &= \sin \Phi \sin 2i \cos \varepsilon + (\cos^2 i - \sin^2 i \sin^2 \Phi) \sin \varepsilon. \end{aligned}$$

And taking the effects of reflexion and refraction into consideration the amplitude on the earth's surface is given by

$$\left. \begin{aligned} u_{11} &\propto \frac{1}{t_P} \Pi \left( \frac{\mathfrak{U}'}{\mathfrak{U}} \right) \left( \frac{u}{\mathfrak{U}} \right)_0 \{ \sin 2i \sin \Phi \cos \varepsilon + (\cos^2 i - \sin^2 i \sin^2 \Phi) \sin \varepsilon \}, \\ u_{12} &\propto \frac{1}{t_P} \Pi \left( \frac{\mathfrak{U}'}{\mathfrak{U}} \right) \left( \frac{w}{\mathfrak{U}} \right)_0 \{ \sin 2i \sin \Phi \cos \varepsilon + (\cos^2 i - \sin^2 i \sin^2 \Phi) \sin \varepsilon \}. \end{aligned} \right\} \quad (83)$$

Taking now tentatively the hypocentre at

$$\varphi = 34^\circ 30' \text{ N}, \quad \lambda = 136^\circ 54' \text{ E}, \quad h = 303 \text{ km.}$$

and putting  $\varepsilon = 25^\circ$ , we obtain the numerical values tabulated in Table XV, and is shown as loci of equal amplitude in Fig. 12.

From this figure we see that the direction and amplitude distributions of this earthquake are well explained also by mechanism of model  $B$ , but comparing with Fig. 11 we can perceive no preference of model  $B$ , though the large amplitudes at Numadu and Kôhu are somewhat better explained by the model  $B$ . These circumstances do not change if we compare more closely by making comparison diagrams of observed amplitude and calculated amplitude (deduced by interpolation and listed in Table XVIII) for each mechanism (see Fig. 13 and 14). We see in the figure that deviations of amplitudes at Numadu and Kôhu from the

Table XV. Calculated amplitude of horizontal component of *P*-wave on the earth's surface due to mechanisms of model *B* for the Ise-bay earthquake.

$$\sigma_{111} = \frac{1}{t_P} \Pi \left( \frac{\mathcal{U}'}{\mathcal{U}} \right) \left( \frac{u}{\mathcal{U}_0} \right) \{ \sin 2i \sin \Phi \cos \varepsilon + (\cos^2 i - \sin^2 i \sin^2 \Phi) \sin \varepsilon \} \times 10^7.$$

$\theta$ $\Phi$	0°	1° 8'	2° 14'	3° 18'	4° 20'	5° 22'	6° 23'	7° 23'	8° 23'	9° 23'	10° 23'
-90°	0	1497	1900	1191	530	70	-212	-380	-542	-551	585
-75°	0	1468	1865	1178	357	89	-186	-350	-509	-519	-553
-60°	0	1383	1756	1132	574	135	-119	-272	-418	-431	-464
-45°	0	1243	1565	1033	537	184	-34	-168	-291	-306	-337
-30°	0	1050	1282	859	466	203	36	-66	-160	-174	-198
-15°	0	813	905	590	334	160	58	-3	-54	-62	-76
0°	0	542	442	232	98	36	11	+ 1	+ 1	+ 3	+ 8
15°	0	255	- 80	- 227	- 224	- 167	-110	- 60	- 3	+ 15	+ 44
30°	0	- 27	- 620	- 719	- 593	- 429	-289	-177	- 59	- 19	+ 34
45°	0	-281	-1125	-1199	- 987	- 708	-493	-324	-149	- 87	- 8
60°	0	-482	-1539	-1601	-1292	- 958	-681	-464	-244	-162	- 61
75°	0	-612	-1810	-1870	-1545*	-1130	-813	-565	-315	-220	-103
90°	0	-657	-1905	-1965	-1625	-1192	-861	-602	-342	-241	+120

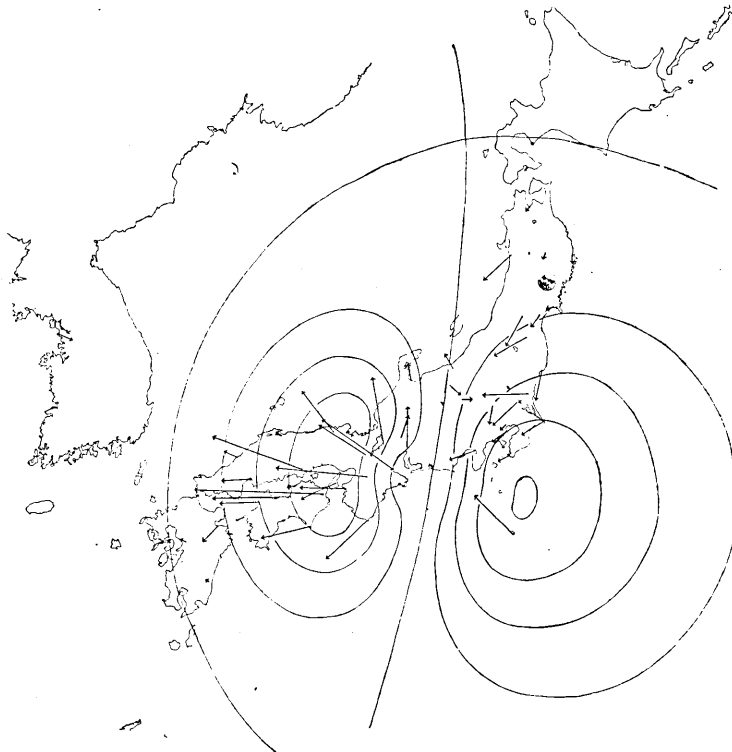


Fig. 12. Distribution of *P* due to the Ise-bay earthquake, and iso-amplitude lines calculated for the mechanism of model *B*.

mechanism of model *A* are not particularly large, and any of the mechanisms will do for the explanation of amplitude of *P*-wave observed in Japan, and we can therefore prefer neither of the mechanisms from the above examinations. So we must examine the *S*-wave.

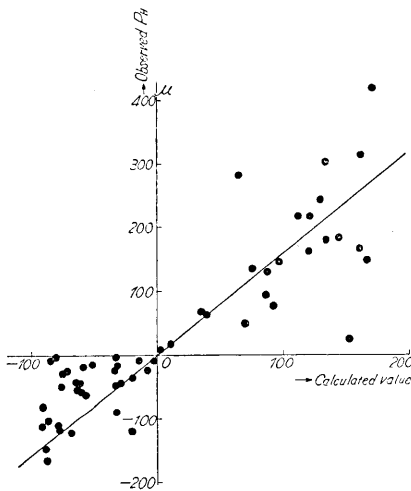


Fig. 13. Comparison of the observed *P* with the value calculated for the mechanism of model *A*.

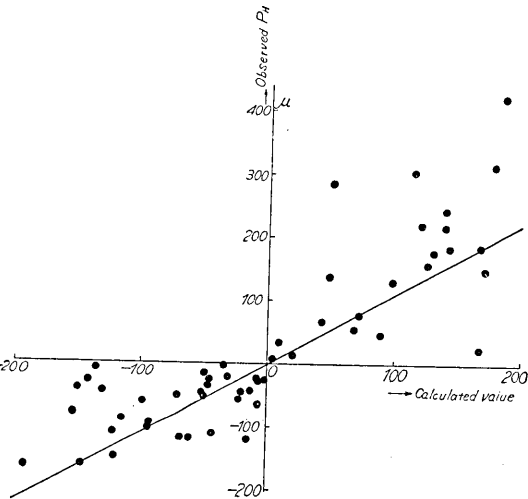


Fig. 14. Comparison of the observed *P* with the calculated value for the mechanism of model *B*.

## 2. Initial Motions of *S*-wave and the Mechanisms of Occurrence of Models *A* and *B*.

The motion due to *S*-wave by the mechanism of model *A* is calculated as in Chapter IV and indicated in Table XVI and Fig. 15. On comparing the figure with the distribution of the observed first motions in Fig. 16, we notice an evident difference. That is the largeness of observed amplitudes in north-eastern part of Japan and the existence of north component motion in the actual observation in the same district, while the nodal line of *S*-wave passes through the district in the above mechanism and direction of motion calculated is nearly westwards. To explain these discrepancies we can superpose any of the *S*-waves of the second kind which may exist independently to the mechanisms by which *P*-waves are generated. For example (Cf. Chapter II, eq. (16))

$$w_3 = C_1 \frac{H_{1+\frac{1}{2}}^{(2)}(kr)}{\sqrt{r}} \sin \theta e^{i\omega t},$$



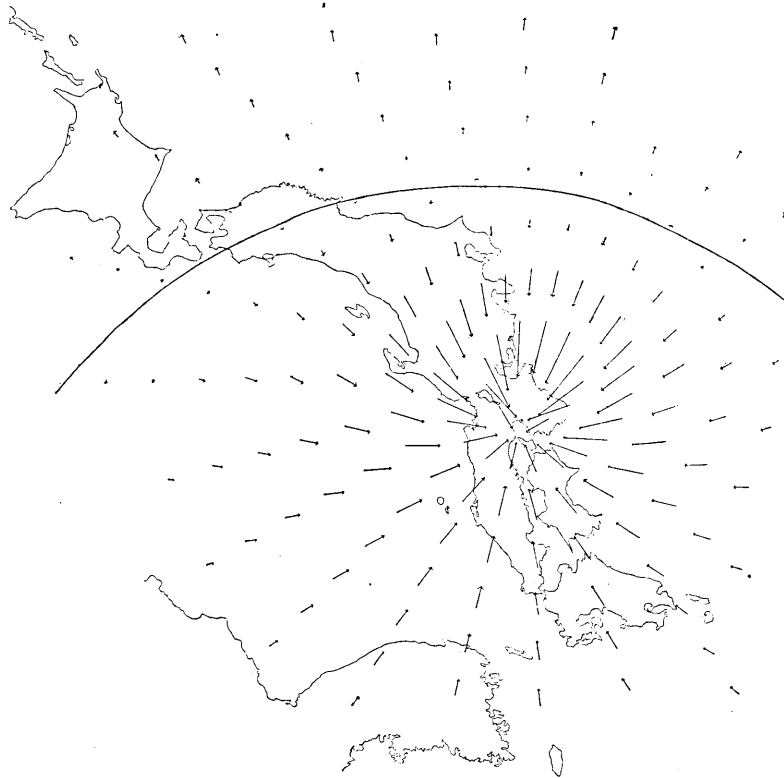


Fig. 15. Distribution of the first horizontal motion of S-wave calculated for model A.



Fig. 16. Distribution of first horizontal motion of S-wave due to the Ise-bay earthquake.

or

$$w_3 = C_2 \frac{H_{2+\frac{1}{2}}^{(2)}(kr)}{\sqrt{r}} \sin \theta \cos \theta e^{i\pi t}, \text{ etc.}$$

And this is convenient to explain the fact found by Mr. Sagisaka that the principal portion of the earthquake motion lasted longer in the Kwantô district (where it is often experienced abnormally severe seismic intensity in case deep-seated earthquake) than the western part of epicentre, because Kwantô and Tôhoku districts are near the equatorial surface  $\theta = \frac{\pi}{2}$  and there may exist such waves which is predominant only near  $\theta = \frac{\pi}{2}$  in the *S*-waves of the second kind independently of *P*-wave.

But if such is really the case and if we superpose only the waves of zonal harmonic amplitude distribution, the displacement must be asymmetrical on both sides of the vertical plane coinciding with the polar axis. Mr. Sagisaka's observation (Fig. 6 of his paper) seems to indicate such relation, as the first motion of *S*-wave at Hatizyôzima is westwards and has no southward component. But examining closely on the seismograms we find a clear southward first motion at *S*-phase of N-S component. And the asymmetry observed above seems to disappear. And in order to explain the fact in this way we must choose *S*-waves of second kind with tesseral harmonic amplitude distribution,<sup>8)</sup> but this will make the problem very complicated.

Then how are the *S*-waves accompanying the *P*-wave of Model *B*? *S*-wave of the first kind accompanying the above *P*-wave is obtained by the relation

$$\sigma_2 = \text{rot rot } \psi e^{i\pi t}$$

from

8) H. KAWASUMI, *Bull. Earthq. Res. Inst.*, 11 (1933), 416.

$$\text{For } n=1=m, \quad u_3=0, \quad v_3 = \frac{1}{2} D \frac{H_{1+\frac{1}{2}}^{(2)}(kr)}{\sqrt{r}} \cos(\varphi + \epsilon) e^{i\pi t},$$

$$w_3 = \frac{-1}{2} D \frac{H_{1+\frac{1}{2}}^{(2)}(kr)}{\sqrt{r}} \cos \theta \sin(\varphi + \epsilon) e^{i\pi t},$$

$$n=2, m=1, \quad u_3=0, \quad v_3 = \frac{1}{6} D \frac{H_{2+\frac{3}{2}}^{(2)}(kr)}{\sqrt{r}} 3 \cos \theta \cos(\varphi + \epsilon) e^{i\pi t},$$

$$w_3 = \frac{-1}{6} D \frac{H_{2+\frac{3}{2}}^{(2)}(kr)}{\sqrt{r}} 3 \cos 2\theta \sin(\varphi + \epsilon) e^{i\pi t},$$

etc.

$$\psi = B \frac{H_{1+\frac{1}{2}}^{(2)}(kr)}{\sqrt{r}} \sin \theta \sin \left( \varphi - \frac{\pi}{4} \right), \dots\dots\dots (84)$$

and this is the same with the *S*-wave in Prof. Hasegawa's model, that is the *S*-wave due to two pairs of double forces, provided  $B_x = -B_y = \frac{iA}{4\mu\sqrt{\pi k}}$  and  $B_z = 0$ , and Prof. Matuzawa's model is obtained by superposing

$$w_3 = B_x \frac{H_{1+\frac{1}{2}}^{(2)}(kr)}{\sqrt{r}} \sin \theta e^{i\gamma t} \dots\dots\dots (85)$$

to the above wave, or from  $\psi = B_x \frac{H_{1+\frac{1}{2}}^{(2)}(kr)}{\sqrt{r}} \sin \theta \sin \varphi^9$ ,  $\left( B_z = \frac{iX}{4\mu\sqrt{2\pi k}} \right)$ . (85) is *S*-wave of the second kind and we may superpose any other kind of *S*-wave of the second kind, but for simplicities sake we shall only consider in the following the types of Professors Hasegawa and Matuzawa. Of course relative magnitudes of *P*- and *S*-waves are subject to the mechanism of occurrence, and we must examine it from the actual observations.

Let us first consider the type of Prof. Matuzawa, which is, as we have seen in Chapter II,

$$\left. \begin{aligned} u_2 &= B \frac{H_{2+\frac{1}{2}}^{(1)}(kr)}{r^{\frac{3}{2}}} \frac{3}{2} \sin^2 \theta \sin 2\varphi e^{i\gamma t} \approx O\left(\frac{1}{r^2}\right), \\ v_2 &= B \frac{1}{r} \frac{d}{dr} \left\{ \sqrt{r} H_{2+\frac{1}{2}}^{(2)}(kr) \right\} \frac{1}{2} \sin \theta \cos \theta \sin 2\varphi e^{i\gamma t} \\ &\approx \sqrt{\frac{2k}{\pi}} B \frac{e^{i(\gamma t - kr)}}{r} \frac{1}{2} \sin \theta \cos \theta \sin 2\varphi, \\ w_2 &= -B \left\{ \frac{k H_{2+\frac{1}{2}}^{(2)}(kr)}{\sqrt{r}} \sin^2 \varphi + \frac{1}{r^{\frac{3}{2}}} H_{2+\frac{1}{2}}^{(2)}(kr) \cos 2\varphi \right\} \sin \theta e^{i\gamma t} \\ &\approx \sqrt{\frac{2k}{\pi}} B \frac{e^{i(\gamma t - kr)}}{r} \sin \theta \sin^2 \varphi. \end{aligned} \right\} (86)$$

There is a nodal plane  $\varphi = 0$  or  $\pi$ . And this is coincident with one of the nodal planes of *P*-wave and corresponds to the so-called fault plane. But in this earthquake no difference could be found by Mr. Sagisaka between the two nodal lines and near both of them large *S*-wave was

9) In Chapten II, the author mistook in identifying this (i. e. eq. (32)) with the *S*-wave in Prof. Hasegawa's model instead of Prof. Matuzawa's. See supplementary note p. 854.



$$\begin{aligned}
 w_3 &= B \frac{1}{r} \frac{d}{dr} \left\{ \sqrt{r} H_{2+\frac{1}{2}}^{(2)}(kr) \right\} \sin \theta \cos 2\varphi e^{i\omega t} \\
 &\approx -\sqrt{\frac{2k}{\pi}} B \frac{e^{i(\omega t - kr)}}{r} \sin \theta \cos 2\varphi,
 \end{aligned}
 \quad \Bigg)$$

is of large amplitude near both of the nodal planes of  $P$ -wave (i. e.  $\varphi = i\frac{\pi}{2}$ ,  $i=0, 1, 2, 3$ ) so we shall calculate the motion similarly as before to see how the observed  $S$ -wave is explained by this formulae. As I

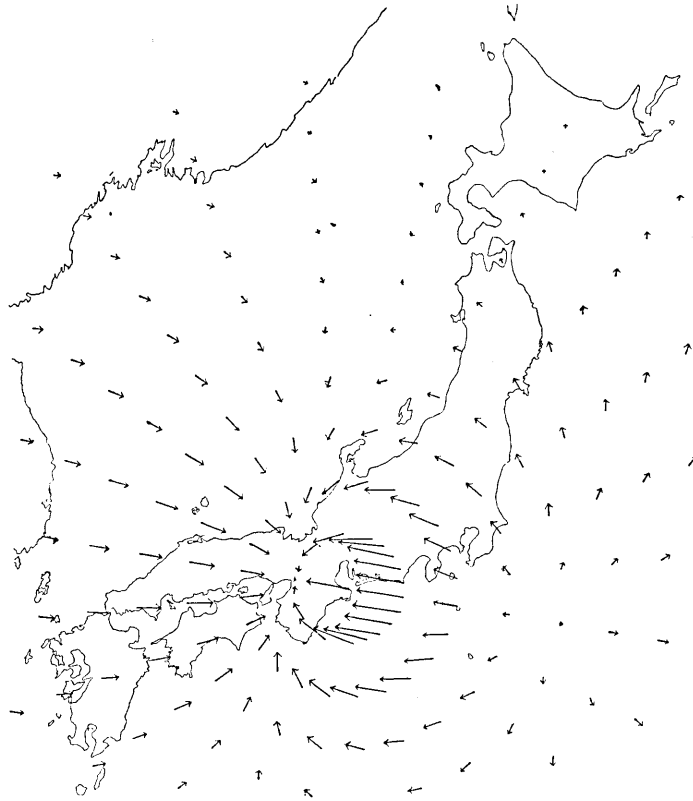


Fig. 17. Distribution of calculated horizontal motion of  $S$ -wave due to mechanism of model  $B$  for the Ise-bay earthquake.

have stated in Chapter II, (87) is equivalent to the waves generated by the two pairs of doublet without moment with different signs, which are perpendicular with each other. Waves due to each pair of doublet was calculated as in the mechanism of model  $A$ . These two parts

are superposed and listed in Table XVII, and the horizontal component vectors are indicated on a map which is shown in Fig. 17. From this we see that the displacement in the western part of epicentre does not differ, as expected, materially from that of model *A*, but eastern part is quite different and the observed displacement of *S*-wave of this earthquake is sufficiently explained. Thus on the contrary to the earthquake seen in Chapter IV, the earthquake here concerned is explained more simply by the mechanism of model *B* of Prof. Hasegawa's type than the mechanism of model *A* in combination with *S*-waves of second kind. And we conclude in this sense, with Mr. Sagisaka, that the earthquake is originated according to the mechanism of model *B*. If we have the observations throughout the world we may be able to conclude with confidence, but with limited observations within Japan we can only reach to the above conventional conclusion.<sup>10)</sup>

### 3. Amplitudes of *P*- and *S*-waves and the Mechanism of Earthquake Occurrence.

Now let us proceed to quantitative examination, calculating the amplitudes for respective stations and compare them with the observed values (Table XII and Table XVIII). In the comparison diagram (Fig. 18), the observed amplitudes by means of Wiechert seismographs are denoted by ● and those of Omori or simple tromometers are denoted by ▲, and between these two groups is observed a clear difference. But owing to the conditions of beginning of motion, the recorded first motion is the smaller the shorter the proper period of seismograph and the larger the damping, and

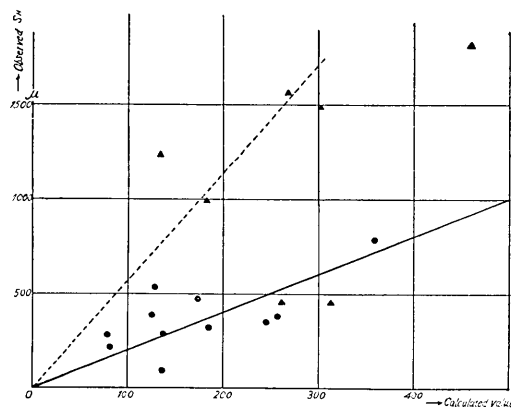


Fig. 18. Comparison of the observed first horizontal motion of *S*-wave due to the Ise-bay earthquake with the calculated value for the mechanism of model *B*.

10) Through the kindness of Prof. M. Ishimoto the writer executed with Mr. R. Yoshiyama such a study of the earthquake of Feb. 20, 1931 from the observations throughout the world. [*Proc. Imp. Acad.*, 10 (1934), 345~348] and we could have evidences which could not be explained by no other mechanism than model *B*.

Table XVIII. Calculated amplitudes of *P*- and *S*-waves of the Ise-bay earthquake for every stations.

	Model A			Model B						
	$\Delta$	$\bar{\Phi}$	$\frac{w_{11}}{\times 10^4}$ ( <i>P</i> <sub>11</sub> )	$\Delta$	$\bar{\Phi}+90^\circ$	$\frac{w_{11}}{\times 10^4}$ ( <i>P</i> <sub>11</sub> )	$\frac{\sigma_{21}}{\times 10^4}$	$\frac{\sigma_{22}}{\times 10^4}$	$\frac{\sigma_{211}}{\times 10^4}$ ( <i>S</i> <sub>11</sub> )	( <i>P</i> <sub>11</sub> )/ ( <i>S</i> <sub>11</sub> )
Tu	30	54.9	64	24	26.6	48	391	-240	459	0.10
Sionomisaki	1 10	-47.2	134	1 24	-57.9	129	0	-325	329	0.39
Hamamatu	55	139.4	35							
Sumoto	2 30	-6.5	158	1 40	-14.6	185	-40	-69	79	2.34
Yagi	55	10.7	133	54	-10.7	114				
Nagoya	56	89.4	75	40	84.7	47	+27	-544	545	0.09
Gihu	1 09	79.0	92	54	73.1	71				
Kyôto	1 09	31.2	144	1 05	11.7	142	115	-88	145	1.00
Hikone	1 09	56.5	121	1 05	45.4	119				
Wakayama	1 24	-11.0	168	1 27	-20.1	170				
Numadu	1 55	143.3	-32	1 46	148.9	-115	-252	-255	359	0.32
Takayama	1 55	91.3	43	1 41	70.3	105				
Tokushima	1 59	-15.6	171	2 25	105.6	-183				
Toyooka	2 00	28.7	160	2 0	22.0	184	-120	-65	137	1.34
Mera	2 26	154.6	-71	2 26	161.7	-130	-125	-120	173	0.75
Hatidyo-jima	2 50	193.9	-88	2 50	160.2	-192	-51	-117	128	1.50
Okayama	2 30	-0.4	161	2 30	-1.1	177				
Niihama	3 06	-15.2	111	3 06	-22.4	138				
Yokohama	2 26	142.8	-62	2 26	147.1	-150				
Oiwake	2 16	114.6	-20	2 16	116.0	-47				
Muroto	2 35	-34.5	120	2 35	38.8	146				
Kumagaya	2 38	127.7	-57	2 38	129.7	-99				
Tokyo	2 50	138.9	-75	2 38	142.5	-142				
Husiki	2 18	84.9	39	2 18	83.0	67				
Nagano	2 41	105.2	-30	2 25	105.6	-13	-78	-309	319	0.09
Mito	3 41	133.6	-88	3 28	135.9	-120				
Tukubasan	3 21	133.0	-91	3 08	135.3	-121				
Kôti	2 48	-24.5	129	2 56	-27.0	139	-215	-158	267	0.52
Yamagata	4 55	114.8	-78	4 41	115.4	-43	41	-125	132	0.33
Tadotu	2 30	-13.7	152	2 36	-15.4	167				
Kakioka	3 25	133.6	-85	3 05	139.1	-136				
Tyôsi	3 39	145.0	-91	3 27	148.2	-153				
Takada	3 43	102.4	-63	2 47	102.7	-7	-52	-254	259	0.03
Utunomiya	3 26	126.4	-81	3 12	108.5	-35				
Matuyama	3 23	-18.8	87	3 30	-20.3	98				
Hirosima	3 35	-6.8	86	3 40	-8.7	94				
Hamada	3 57	1.4	69	4 00	-2.2	72	-257	-3	257	0.28
Hukushima	4 35	109.5	-77	4 20	120.6	-61				

(to be continued.)

Table XVIII. (continued.)

	Model A			Model B						
	$\Delta$	$\bar{\varphi}$	$\frac{w_{11}}{\times 10^4}$ ( $P_n$ )	$\Delta$	$\bar{\varphi}+90^\circ$	$\frac{w_{11}}{\times 10^4}$ ( $P_n$ )	$\sigma_{21}$ $\times 10^4$	$\sigma_{22}$ $\times 10^4$	$\frac{\sigma_{21}}{\times 10^4}$ ( $S_n$ )	$\frac{(P_n)}{(S_n)}$
Onahama	4 17	130°	-87	4 04	131°	-94				
Ôita	4 26	-22°9	35	4 34	-24°8	42				
Sendai	5 12	118°5	-76	4 57	119°4	-50	54	-113	125	0.40
Isinomaki	5 32	119°9	-72	5 18	120°8	-46				
Miyazaki	5 05	-36°5	2	5 16	-38°2	20	-182	-10	182	0.11
Simonoseki	4 52	-14°3	25	4 58	-15°5	10				
Hukuoka	5 20	-17°0	10	5 27	-17°9	6				
Kumamoto	5 17	-17°9	10	5 26	-26°5	9				
Unzen-dake	5 40	-24°1	-3	5 49	-25°8	3				
Nagasaki	5 58	-23°0	-8	6 07	-28°8	-8	-183	28	185	0.04
Akita	6 02	105°1	-68	5 47	105°3	-15	30	-76	81	0.19
Morioka	6 28	111°5	-63	6 13	111°9	-20				
Miyako	6 47	116°2	-61	6 33	116°8	-22				
Aomori	7 17	102°4	-59	7 02	104°6	-7				
Taiikyû	6 53	5°9	-15	6 55	3°7	-31				
Titi-zima	8 33	-134°3	-33	8 42	-132°9	-12	100	-79	127	0.09
Hakodate	8 08	101°2	-52	7 52	101°3	-2				
Keizyô	8 35	15°3	-32	8 35	13°7	-50				
Zinsen	9 01	16°8	-33	8 49	12°8	-52	-130	40	136	0.38
Kôhu	2 01	125°9	-20	1 47	129°7	-68				
Kanazawa	2 18	77°3	48	2 02	74°3	89	-84	-290	302	0.29
Hukui	1 52	67°1	98	1 39	61°8	125	-46	-310	314	0.40

such difference as in Fig. 18 is not improbable. If we determine the constant connected with the amplitude of  $S$ -wave from the data due to Wiechert seismographs we obtain (from the straight line in Fig. 18)

$$2\mu = B \sqrt{\frac{2k}{\pi}} \frac{1}{a} \times 10^{-4},$$

in which  $\bar{a}$  (mean velocity of  $P$ -wave) = 7.63 km./sec. On the other hand we have as the coefficient of  $P$ -wave from Fig. 14,

$$1.1\mu = A \sqrt{\frac{2h}{\pi}} \frac{1}{a} \times 10^{-4}.$$

If the earthquake is generated exactly according to the mechanism of model  $B$  of Prof. Hasegawa's type the maximum amplitudes of  $P$ - and  $S$ -waves at the same hypocentral distance will be inversely proportional to the cube of their velocities, and the  $S$ -wave must be about 5.2 times

of  $P$ -wave in the Poisson's hypothesis. And it is necessary in such case to become

$$5.72\mu = B \sqrt{\frac{2k}{\pi}} \frac{1}{a} \times 10^{-4}.$$

This relation is denoted in Fig. 18 by a broken line which passes through the points  $\blacktriangle$  due to Omori or simple tromometer.

Strictly speaking the comparison of data obtained by means of seismographs with different instrumental constants without proper corrections is absurd, so let us

now consider the ratio of amplitudes of  $P$ - and  $S$ -waves at the same station by the same instrument. Then this value will be better even if we do not apply the corrections due to initial conditions. The observed and calculated ratios of horizontal components of  $P$ - and  $S$ -waves ( $P_H/S_H$ ) are compared in Fig. 19. We can see from the figure that the observed ratios are large in

general more than two times of the relation in Prof. Hasegawa's model (observed ratio  $\times 5.2 =$  calculated value). This is also in harmony with the result already stated.

Such tendency as above that the  $S$ -wave becomes smaller may happen if there is damping due to solid viscosity<sup>11)</sup> in the material consisting the earth's crust, but if such large effect as above is to be explained in this way, we should expect large diminution of amplitudes of  $P$ - and  $S$ -waves with epicentral distance and the ratio  $P_H/S_H$  should also increase with the same distance. But we cannot observe such a systematic variation. Therefore the explanation of the fact as the effect of damping is impossible, and we must conclude that the earthquake was generated by somewhat different mechanism than Prof. Hasegawa's type.

#### 4. Energy emitted from the Hypocentre as Seismic Waves.

Lastly we shall consider the energy carried out by seismic waves

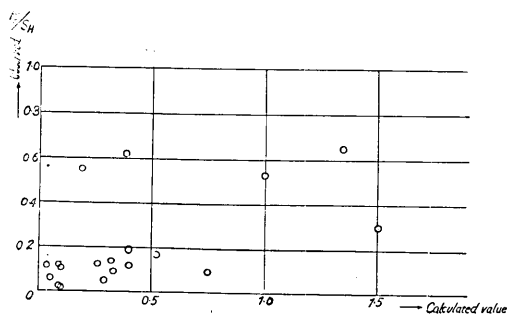


Fig. 19. Comparison of the ratio of horizontal component of first motions of  $P$ - and  $S$ -waves due to the Ise-bay earthquake with the calculated value for the mechanism of model B.

11) K. SEZAWA and K. KANAI, *Bull. Earthq. Res. Inst.*, 10 (1932), 299-334.

from the hypocentre. From the constants obtained above, the displacements at large distance from the hypocentre are (taking the real part)

$$\left. \begin{aligned}
 u_1 &= -1.1 \bar{a} \frac{\cos(pt - hr)}{r} \sin^2 \theta \sin 2\varphi \text{ cm.} \\
 &= -8.4 \frac{\cos(pt - hr)}{r} \sin^2 \theta \sin 2\varphi \times 10^5 \text{ cm.,} \\
 v_2 &= -2 \bar{a} \frac{\cos(pt - kr)}{r} \sin \theta \cos \theta \sin 2\varphi \text{ cm.} \\
 &= -15.3 \frac{\cos(pt - kr)}{r} \sin \theta \cos \theta \sin 2\varphi \times 10^5 \text{ cm.,} \\
 w_2 &= -2 \bar{a} \frac{\cos(pt - kr)}{r} \sin \theta \cos 2\varphi \text{ cm.} \\
 &= -15.3 \frac{\cos(pt - kr)}{r} \sin \theta \cos 2\varphi \times 10^5 \text{ cm.}
 \end{aligned} \right\} \dots (88)$$

As I have shown in Chapter IV, the energy flowing out in one period  $T$  from a sphere  $r = \text{const.}$  (say  $c$ ) is constant not with-standing the value of  $c$ , and we may calculate the energy using the displacement at large distance neglecting  $1/r^2$  in comparison of  $1/r$ . By means of the formula

$$E = \int_0^T dt \int_0^{2\pi} d\varphi \int_0^\pi \{ \dot{u}r + \dot{v}r\theta + \dot{w}r\varphi \} r^2 \sin \theta d\theta^{12)} \dots (89)$$

and (88), the energy  $E_u$  and  $E_t$  for  $P$ -wave ( $u_1$ ) and  $S$ -wave ( $v_2, w_2$ ) respectively are calculated separately.

$$-E_u = \frac{16}{15} \pi^2 \rho a p \times (8.4 \times 10^5)^2,$$

$$-E_t = \frac{8}{5} \pi \rho b p \times (15.3 \times 10^5)^2,$$

and taking  $T = 4$  sec. velocity of longitudinal wave  $a = 8.4$  km./sec. the velocity of transverse wave  $b = 4.87$  km./sec., and  $\rho = 3.8$ , we obtain

$$-E = 0.37 \times 10^{23} \text{ ergs.} \quad \text{and} \quad -E_t = 1.07 \times 10^{20} \text{ ergs.}$$

As we have used for the amplitude the first motion on seismogram without correction, the actual amplitude must be about twice as large, so the actual energy will be about  $2^2 = 4$  times of the above values.

---

12) The formulae  $E = \int (uX_s + vY_s + wZ_s) dS$  and (66) in Chapter IV were misprinted.  $u, v$  and  $w$  in these formula should be replaced by  $\dot{u}, \dot{v}$  and  $\dot{w}$  respectively.

(Besides the energy of  $S$ -wave due to mechanism of Prof. Hasegawa's type corresponding to the above  $P$ -wave is  $-E_t=8.75 \times 10^{20}$  ergs.)

Mr. Sagisaka obtained by the graphical integration the energy within about one wave length (or carried away in 4 sec.)

$$-E_l=1.34 \times 10^{20} \text{ ergs. and } -E_t=10.63 \times 10^{20} \text{ ergs.}$$

using maximum amplitudes in  $P$ - and  $S$ -phases, without taking into consideration the effect of reflexion at the earth's surface, so the above energy must be about  $2^2=4$  times of the actual if though the maximum amplitude used by him is the actual amplitude of ground motion.

The mean amount of energy carried out from the hypocentre in one second by both of  $P$ - and  $S$ -waves is

$$R = -\frac{E}{T} = -\frac{E_l + E_t}{T} = 3.7 \times 10^{19} \text{ ergs.}$$

And this is a little larger than that of the Central Japan earthquake of June 2, 1931 ( $R=2.7 \times 10^{19}$  ergs). In the actual seismogram we see that motion with amplitude of the same order as the first motion lasted more than 10 seconds, so the total energy carried out as seismic waves from the hypocentre of this earthquake was the order of  $10^{21}$  ergs.

##### 5. Concluding Remark of Chapter V.

From the above study we see that the distribution of first motions of  $P$ - and  $S$ -waves due to the Ise-Bay earthquake of June 2, 1929 are most easily explained by the mechanism of model  $B$ , confirming the opinion of Mr. Sagisaka. The mechanism of model  $A$  suggested by Prof. Ishimoto is also sufficient to the explanation of  $P$ -wave, and the explanation of the first motion of  $S$ -wave by this mechanism is not impossible if we superpose some kinds of  $S$ -waves of second kind. The difference in fitness of the two mechanisms is slight.

Then considering that the earthquake was generated by the mechanism of model  $B$ , the position of hypocentre came out at about  $\varphi=34^\circ 30' \text{ N}$ ,  $\lambda=136^\circ 54' \text{ E}$  and  $h=\text{ca. } 300 \text{ km}$ . The direction in which  $P$ -wave was of maximum amplitude and the initial motion is compressional is inclined at the hypocentre at about  $33^\circ$  from the seismic vertical in the azimuth  $\text{NS}0^\circ \text{W}$ . The wave emitted in this direction seems to have reached in the vicinity of Osaka, but unfortunately we have no observations at Osaka and Kôbe. If we were able to observe at these stations, the seismograms obtained there would have shown no preliminary tremor as Prof. Omori found at these stations in the earthquake of Feb. 1, 1907 (this earthquake was probably originated off the coast of Ensyû

by the same mechanism as the above earthquake). The large amplitude of *P*-wave at Kyôto, Sumoto, Wakaura and Hikata will show this circumstance.

From the observation of *S*-wave we can see that the earthquake is not a so-called fault earthquake of Prof. Matuzawa's type but is nearly that of Prof. Hasegawa's model. But closely studying the ratio of amplitudes of *P*- and *S*-waves we must conclude that the *S*-wave is a little smaller than in the model of Prof. Hasegawa, but the explanation of this fact by the damping due to viscosity is probably impossible. Lastly the energy carried out as seismic waves from the hypocentre came out in the mean,  $3.7 \times 10^{19}$  ergs per second, and the total of such energy may be of the order of  $10^{21}$  ergs.

#### Chapter VI. "Pull-push" Distribution of Initial Motions of Earthquake of Shallow Origin and Structure of Earth's Crust.

As already stated in Chapter I, there are a number of studies concerning the mechanism of occurrence of earthquake of shallow origin as seen from the "pull-push" distribution of initial motions. But there remain important problems, and from whose examination it is promised the solution of some important questions. In the following I will only make clear of these points by a few examples, and final conclusion is a matter of future studies.

According to the former studies the mechanism of occurrence of earthquake of shallow origin seems to be hardly different from those of deep-seated earthquakes which have been seen in preceding chapters. But the difficulties in the study of the former compared with that of deep-seated earthquake are due to the proximity of the hypocentre from the observing stations which makes the space derivatives of the phenomena to become large apparently, and in consequence, it is difficult to catch the whole phenomena even with the seemingly dense net of observing stations in Japan, besides small irregularities in the structure of the earth's crust may possibly cause the large difference in the earthquake motions. But on the other hand the largeness of space derivative serves a very important clue for the determination of crustal structures. Indeed, even the shape of nodal lines shows fine correspondence with crustal structure.

##### 1. *On the Existence of Discontinuity Surface in the Earth's Crust*

as inferred from the Shape of Nodal Lines.

As an example let us see the earthquake of July 27, 1929 which originated in the middle part of Sagami province. Mr. Hayata<sup>13)</sup> already

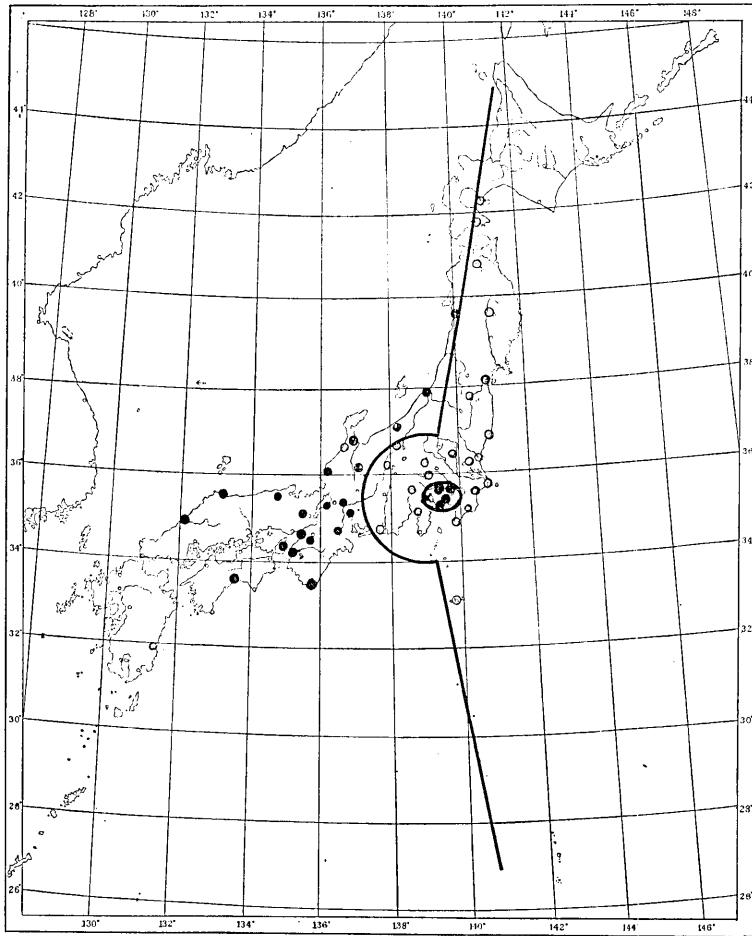


Fig. 20. "Pull-push" distribution of the earthquake of June 27, 1929.

- compression = push
- dilatation = pull

studied this earthquake in detail, and gave the direction of initial motion in his paper, but he did not discuss the mechanism of the earthquake occurrence. Plotting his observations as well as the observations

13) K. HAYATA, *Geophys. Mag.*, 4 (1931), 39~51.

at stations in Kwantô plain under the Earthquake Research Institute<sup>14)</sup> on a map, we find peculiar "pull-push" distribution (Fig. 20). Near the epicentre there is an isolated group of stations (Tôkyô, Yokohama, Mitaka and Kamakura) where the first motions of  $P$ -wave were compressional (or push), and the surrounding stations recorded first a dilatation. And this again changes into a region in the western part of epicentre where the stations again recorded first a compression. But in the northern part of epicentre Niigata and Akita recorded first a compression while Hukusima, Sendai, Morioka, Aomori, Hakodate and Muro-ran recorded first a dilatation. The boundary between these regions is very remarkable. It is nearly straight line in the northern part and nearly circular in the western part of the epicentre. It is difficult to explain the "pushes" in the vicinity of Tôkyô by no other mechanism than model  $A$ , and the boundary curve of the western and northern parts can also be interpreted if we assume discontinuity surface in the earth's crustal structure by the same mechanism, while, on the contrary, it is very difficult to explain the fact by assuming a continuous variation of velocity within the crust here concerned, as in the model of Messrs. Sagisaka<sup>15)</sup> and Honda<sup>16)</sup> which was obtained under the assumption that nowhere two seismic rays of the same kind of wave reach from the hypocentre. The circular arc in the western part is interpreted then as the circle at which  $P$ - and  $\bar{P}$ - (say) waves arrives at the same time (which is the so-called inflexion circle<sup>17)</sup> named by Dr. K. Wadati, but I am not sure of its appropriateness, so it will be called in this paper provisionally a critical circle), and transition from the inner region to the outer of this circle means a discontinuous change in the emergency angle, and this circular boundary is not primary nodal line, but it is a secondary one due to singularity in the structure of the earth's crust.

But we may not necessarily assume the existence of discontinuity surface to explain the shape of the nodal line, but it is very difficult to elucidate it by assuming continuous variation of velocity and uniqueness of seismic ray of  $P$ -wave from a hypocentre to a station.

Let us now make clear of these points taking the present know-

---

14) Seismometrical Report of Earthquake Research Institute, 1924~1930 (1934).

15) K. SAGISAKA, *Geophys. Mag.*, 4 (1931), 147-155.

16) H. HONDA, *Geophys. Mag.*, 4 (1931), 29-38; *ibid.*, (1931), 185-213.

17) K. WADATI, *Geophys. Mag.*, 1 (1927), 89-96.

S. I. KUNITOMI, *do.*, 1 (1928), 238-254; *do.*, 3 (1930), 149-164.

ledge of crustal structures into consideration. As to the crustal structures in Japan, since Dr. K. Wadati introduced the single-layer model Messrs. S. I. Kunitomi,<sup>18)</sup> K. Sagisaka, H. Satô,<sup>19)</sup> K. Hayata<sup>20)</sup> and T. Hirano<sup>21)</sup> followed Dr. Wadati, but T. Matuzawa<sup>22)</sup> introduced two-layer model, while Messrs. K. Sagisaka and Honda denied the existence of discontinuity surface near the earth's surface, and Dr. Wadati<sup>23)</sup> adopted the hypothesis. All these hypotheses are now to be examined.

Mr. Hayata who studied this earthquake assuming the single-layer model worked out that the depth of hypocentre of this earthquake, and the thickness of the crustal layer to be 23 km. and 42 km. respectively, and velocity of  $P$ -wave above and below the boundary of the layer to be 5.6 and 7.5 km./sec. while the radius of the critical circle was 165 km. Adopting these values we obtain the nodal lines as shown in Fig. 20 if we assume the distribution of initial motion of  $P$ -wave to be  $P_2(\cos\theta)$  whose polar axis is inclined eastwards by about 20°. This figure affords perfect elucidation of the observed result.

Now then, the two-layer model of Prof. Matuzawa will be examined. As Mr. Hayata observed  $P$ -wave of this earthquake we must take hypocentre within the first layer. According to Prof. Matuzawa the thickness of the first layer is 20 km. and velocity in which is 5.0 km./sec., while those for the second layer are 30 km. and 6.1 km./sec. and the velocity in the subcrust is 7.5 km./sec. Then the radius of the critical circle (that is the distance where  $\bar{P}$ - and  $P^*$ -waves arrive at the same time) is at most 127 km. even when the hypocentre lies on the earth's surface, which is decidedly smaller than the observed value, but to explain the "pushes" in the vicinity of Tôkyô and Yokohama we must assume finite hypocentral depth. Therefore we cannot explain the observed radius of the critical circle by that of  $\bar{P}$ - and  $P^*$ -waves. On the other hand if we are to explain it by that of  $P^*$ - and  $P$ -waves, the minimum radius of critical circle is 210 km. so far as the hypocentre is within the first layer. Of course our endeavours of determining the crustal structure become absurd if the dimension of hypocentre is considerably large, because we can then determine it by neither of the consideration of the mechanism of earthquake occurrence nor observation

18) S. I. KUNITOMI, *loc. cit.*, and *Geophys. Mag.*, 2 (1929), 65~89.

19) K. A. SAGISAKA and H. SATO, *Journ. Met. Soc., Japan*, [ii], 4 (1926), 301~307.

20) K. HAYATA, *loc. cit.*, and *Journ. Met. Soc. Japan*, [ii], 7 (1929), 302~310.

21) T. HIRANO, *Kensin Zihô*, 3 (1931), 243~290.

22) T. MATUZAWA, *Bull. Earthq. Res. Inst.*, 5 (1928), 1~28; 6 (1929), 171~229.

23) K. WADATI and S. OKI, *Geophys. Mag.*, 7 (1933), 113~153.

of travel times. So it is of some importance to examine the "pull-push" distribution to verify these circumstances.

How then is the model with no discontinuity surface due to Messrs. Sagisaka and Honda which was worked out from the assumption of uniqueness of seismic ray of *P*-wave from hypocentre to a station? For this model Dr. Wadati<sup>24)</sup> and others have culculated time distance curves and cosines of emergency angles for earthquakes of various hypocentral depths. So we can calculate the shape of nodal lines just in the same way as in preceding chapters. In cases of hypocentral depths less than 20 km. or larger than 60 km., nodal lines near the epicentre and western boundary curve at about 160 km. can never be explained by single system of surface. And only the case of hypocentral depth of 40 km. remains. In this case the backward continuations of seismic rays which generate the boundary surface through Niigata Takada, Takayama and Nagoya sufficiently include the "pushes" near Tôkyô and exclude the "pulls" around them. This new boundary curve represent minimum distance of appearance of nodal line, while the backward continuation of seismic ray reaching Hamamatu, Matumoto, Nagano, Hakodate and Muroran give the upper limits. Narrow strip between these limits are nearly circular in the eastern and southern sides of the epicentre while it suddenly contracts at south-western end. So we can never obtain a nodal line satisfying these conditions as an intersection of the earth's surface with a circular cone surface modified by crustal structures. Changing the hypocentral depth to 30 or 35 km. we could not find no possibility of elucidating the "pull-push" distribution by this model. We must therefore conclude the existence of discontinuous variation of emergency angle with epicentral distance within  $\Delta=200$  km., so far as the "pull-push" distribution of this earthquake is concerned.

From the above example the model of Mr. Hayata is in good accord with the observed results, but we cannot conclude from this alone, because it is not sufficient to elucidate the "pull-push" distribution of the great Kwantô earthquake<sup>25)</sup> of Sep. 1, 1923, which was probably origi-

24) K. WADATI, K. SAGISAKA and K. MASUDA, *Geophys. Mag.*, 7 (1933), 87~99.

25) For the explanation of "pull-push" distribution of this earthquake a number of mechanisms were proposed.

S. T. NAKAMURA, *Rep. Earthq. Inv. Comm.*, 100 (192 ).

T. SHIDA, in M. MATUYAMA's *Bankin no Disingaku* (1925), 235~236.

S. I. KUNITOMI, *Geophys. Mag.*, 3 (1930), 149~164.

M. ISHIMOTO, *Bull. Earthq. Res. Inst.*, 10 (1932); 11 (1933).

From the method of explanation of Mr. Kunitomi the boundary of "pull" and "push" cannot be explained.

nated by the same mechanism with the above example. Though the Kwantô earthquake may be explained with Mr. Hayata's model by assuming larger vertical angle of the nodal cone than those of the earthquakes hitherto considered ( $55^\circ$ ), but we must examine a number of earthquakes before concluding.

The writer told the above view in 1932 to Prof. Ishimoto, who agreed with this and applied it to a number of earthquakes,<sup>26)</sup> and Mr. T. Minakami<sup>27)</sup> studied statistically with the data taken from Kisyô Yôran. And their results (though they are qualitative) are in favour of the above opinion. But we must examine seismograms of individual earthquakes systematically to solve the problem.

2. *Provisional Calculation of Shapes of Nodal Lines for Various Cases as a possible Application of the Fact suggested by the above Example.*

The above problems are so important that the effect of the crustal structures suggested by the above example on the "pull-push" distribution will be examined beforehand for the convenience of verification by the actual examples.

There are a number of cases of "pull-push" distribution in the mechanism of model *A* besides the case denoted in Fig. 20, and in the mechanism of model *B* we also have interesting figures. For simplicities sake a single-layer model is considered. On writing  $d$ ,  $v_1$ ,  $v_2$ , and  $h$  for the thickness, the velocities within and below the surface layer, and hypocentral depth respectively, we have for the radius of the critical circle

$$\Delta_0 = (2d - h) \{ \tan i_1 + \sec i_1 \}, \quad \sin i_1 = v_1/v_2,$$

in which  $i_1$  is the critical angle of incidence of first appearance of *P*-wave. And the seismic ray emitted downwards within the cone with vertical angle  $i_1$  determines the "pull" or "push" in the outer region of the critical circle. The intersection of this cone with the boundary of the layer is a circle of radius  $\Delta_0' = (d - h) \tan i_1$ , and as Mr. Hayata<sup>28)</sup> has remarked, in the azimuths of the intersections of this circle and

26) M. ISHIMOTO, *Bull. Earthq. Res. Inst.*, 11 (1933).

M. ISHIMOTO, "On the distribution of initial motions of earthquakes whose hypocentral depths are less than 50 km." (Lectured at the colloquium of the Seismological Institute on Oct. 18, 1933).

27) T. MINAKAMI, Delivered the results of his study at the meeting of the Earthquake Research Institute on Feb. 20, 1934. (Unpublished).

28) K. HAYATA, *Journ. Met. Soc. Japan*, [ii], 7 (1929), 302~310.

nodal surface appear nodal lines in the outer regions of the critical circle.

First let us consider the mechanism of model *A*. On denoting the inclination of the polar axis from the zenith by  $i_0$ , and vertical angle of nodal cone by  $a$ , and taking  $z$ -axis vertically and  $x$ -axis in the azimuth of polar axis, nodal cone is expressed by

$$(x \cos i_0 + z \sin i_0)^2 + y^2 = \tan^2 a (z \cos i_0 - x \sin i_0)^2.$$

From these equations we can calculate nodal lines on the earth's surfaces.

Now let us consider the mechanism of model *B* in which two nodal planes at right angles appear. The line of intersection of the nodal planes which run through the hypocentre  $H$  is denoted by  $PHP'$ , and normals to these nodal planes through  $H$  are denoted by  $HQ$  and  $HR$ , and intersections of  $HP$ ,  $HQ$  and  $HR$  with the earth's surface are called  $P$ ,  $Q$  and  $R$  respectively, and the angles subtended by these lines with the seismic vertical  $HE$  are represented by  $\alpha$ ,  $\beta$  and  $\gamma$ . And putting  $\angle PEQ = \varphi$ ,  $\angle PER = \psi$ ,  $\angle PQR = \theta$  and  $\angle RPE = \theta'$  (where  $E$  is epicentre), we have the following relations between these angles,

$$\begin{aligned} \cos \varphi &= -\cot \alpha \cot \beta, & \cos \psi &= -\cot \alpha \cot \gamma, \\ \sin \theta &= \frac{\cos \alpha \sin \beta \sin \varphi}{\sin \gamma}, & \sin \theta' &= \frac{\cos \alpha \sin \gamma \sin \psi}{\sin \beta}, \end{aligned}$$

from which we can draw nodal lines. On the other hand we also obtain nodal lines by the relations

$$EP = HE \tan \alpha, \quad EQ = HE \tan \beta, \quad ER = HE \tan \gamma$$

together with the angles  $\varphi$  and  $\psi$ .

On assuming  $d=40$  km. and  $v_1/v_2=5.5/7.5$ , some examples of interest are worked out in Fig. 21 by means of the above relations and some times graphically. The explanation in detail of these diagrams are omitted, and here is given only a notion of Prof. Ishimoto that the portion included within the nodal cone in model *A* records first a compression as indicated in Fig. 21, while the "pulls" and "pushes" due to the mechanism of model *B* may be interchanged in each other.

##### 5. Summary of Chapter VI.

In this chapter the writer intended to reveal that the examination of "pull-push" distribution of earthquakes of shallow origin offers a powerful means of determination of crustal structure, but final result is not attained. As an example the earthquake of June 27, 1928

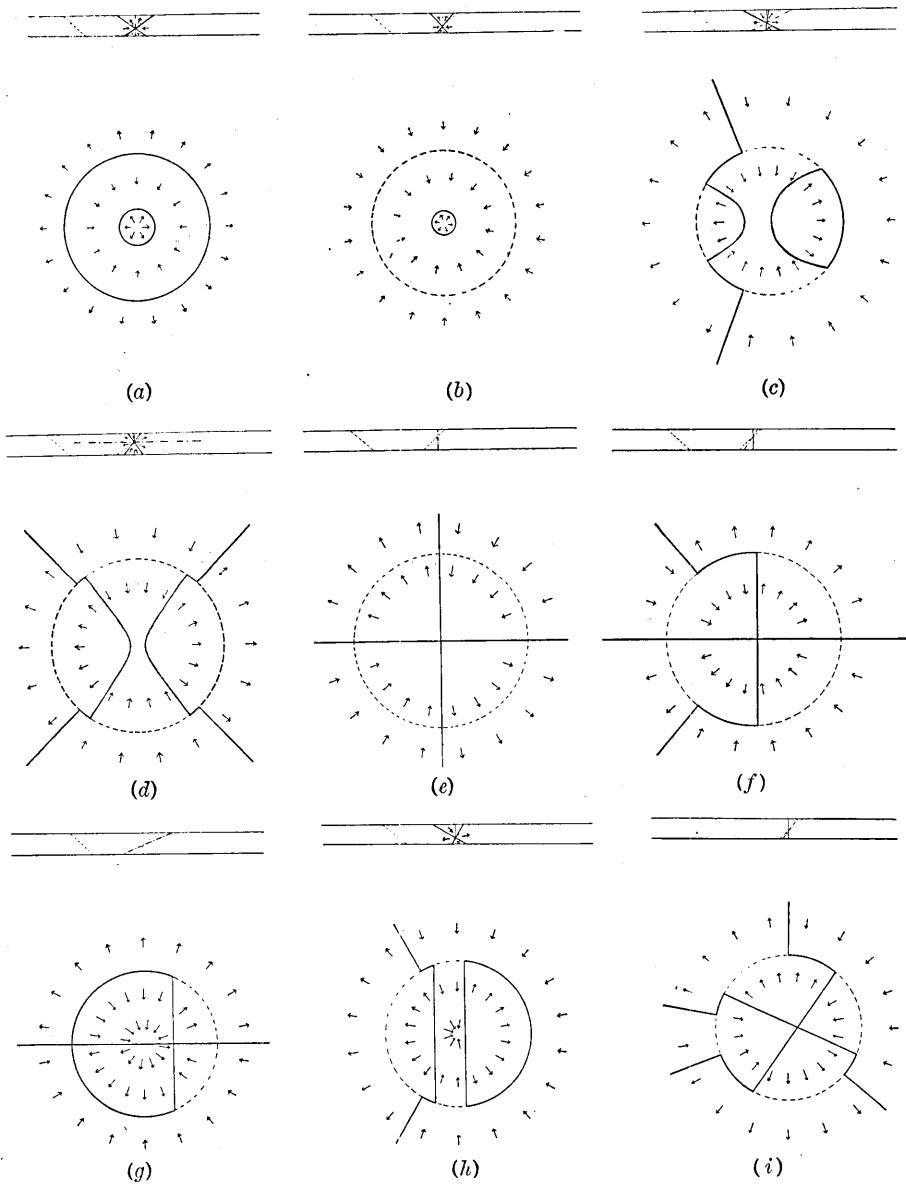


Fig. 21. "Pull-push" distributions on the surface of a single-layer model.

- (a) Model A. The axis of nodal cone is vertical. The vertical angle  $\alpha$  is larger than the critical angle of incidence  $i$ .
- (b) Model A. The axis of nodal cone is vertical.  $\alpha < i$ .
- (c) Model A. The axis of nodal cone is inclined.

- (d) Model A. The axis of nodal cone is horizontal.
- (e) Model B. Two nodal plane is vertical.
- (f) Model B. One of the nodal planes is inclined.
- (g) Model B. One of the nodal planes is vertical, while the other inclines much.
- (h) Model B. Both nodal planes are inclined, the intersection is horizontal.
- (i) Model B. Both nodal planes as well as their intersection are inclined.

originated in the middle part of Sagami province was discussed, from which it was revealed the necessity of assuming the discontinuity in the variation of emergency angle with epicentral distance within  $\Delta$  less than 200 km., and that the single-layer model of Mr. Hayata is capable of elucidating the above example, but necessity of precaution before concluding was noticed by the Great Kwantô earthquake. As a possible application of the result inferred from the above example some cases of "pull-push" distributions of various cases are calculated provisionally.

### Chapter VII. On the Structure of the Earth's Crust near the Surface as viewed from the Magnitude of Initial Motions of Earthquake of Shallow Origin.

#### 1. *The North Idu Earthquake of Nov. 25, 1930, and the Itô Earthquake of Mar. 23, 1930.*

At the meeting of the Meteorological Society of Japan in June, 1931, Mr. H. Honda<sup>29)</sup> delivered a very interesting study of the above earthquakes. He stated that the magnitudes of initial motions of these earthquakes were proportional to

$$\frac{1}{\Delta^2} \sin 2(\varphi + \varepsilon),$$

(where  $\Delta$  and  $\varphi$  denote epicentral distance and azimuth respectively), in agreement with the theoretical result of late Dr. H. Nakano's investigation<sup>30)</sup> of elastic waves in semi-infinite solid generated by tractions on the free surface. He also said that the distribution of amplitudes of S-wave as well as the types of seismograms were also in favour of the above explanation. From this he proceeded to suspect the existence of discontinuity surface near the earth's surface. But this problem is so important that full examination is necessary before concluding. The smallness of the velocity near the earth's surface in comparison with the deeper portions than 50 or 60 km. is a well established fact and

29) H. HONDA, *Geophys. Mag.*, 4 (1931), 185~213.

30) H. NAKANO, *Geophys. Mag.*, 2 (1930), 189~348.

the velocity distribution by Mr. Honda<sup>31)</sup> confirms also this statement. The theoretical result of Dr. Nakano may therefore be applicable only in the region sufficiently near the epicentre but at an infinite distance compared with the wave length. And it is more natural to suspect the applicability of the theoretical result of Dr. Nakano in the region where the waves travelled a roundabout way arrive.

Thus the writer considered how far the observed fact might be explained by taking the heterogeneous crustal structure into consideration. The variation of amplitude with the azimuth found by Mr. Honda is accepted. But is it impossible to elucidate the variation with epicentral distance by the variation of energy density in consequence of the heterogeneity in the crustal structure in combination with the effect of reflexion and refraction? The effects of reflexion and refraction<sup>32)</sup> at a discontinuity surface on the amplitude of seismic waves were not known at that time, the writer therefore considered only the crustal structure with no discontinuity surface deduced by Mr. Honda from the above earthquakes. The method of calculation was the same as stated in Chapter III, the effects of reflexion and refraction at the discontinuity surfaces were neglected.

Following Mr. Honda the hypocentral depths of these earthquakes were assumed to be null. Then the angles  $e_n$  and  $e_o$  in the equation (39) become equal, and the equation reduces to

$$\mathfrak{A}\infty\sqrt{\frac{-d(\cos e_o)}{\sin e_o d(\cos \theta)}} = \sqrt{\frac{1}{\sin \theta} \frac{d(\log \sin e_o)}{d\theta}} \approx \frac{1}{\sqrt{\theta}} \sqrt{\frac{d(\log \sin e_o)}{d\theta}}$$

for small value of epicentral distance  $\theta$ . By virtue of the relation  $R\theta = \Delta$ , where  $R$  is the radius of the earth, we have

$$\mathfrak{A}\sqrt{\Delta}\infty\sqrt{\frac{d(\log \sin e_o)}{d\Delta}}$$

From the table of  $\cos e_o$  with  $\Delta$  of Mr. Honda, the difference of  $\log_{10} \sin e_o$  corresponding 10 km. interval of  $\Delta$  was obtained, and the values per km. thus deduced was used for  $\frac{d(\log \sin e_o)}{d\Delta}$  at the middle point of the interval. If we put

$$\sqrt{\frac{d(\log_{10} \sin e_o)}{d\Delta}} \equiv \sqrt{\Delta} U,$$

31) H. HONDA, *Geophys. Mag.*, 4 (1931), 29~39.

32) H. KAWASUMI and T. SUZUKI, *Disin*, 4 (1932).

$U$  is proportional to the amplitude of incident wave at the surface. Multiplying this by the factor  $\frac{u}{U}$  representing the ratio of amplitude of the surface horizontal motion to that of incident wave in consequent of surface reflexion, we obtain

$$\sqrt{\frac{d(\log_{10} \sin \epsilon_0)}{d\Delta}} \left( \frac{u}{U} \right) \equiv \sqrt{\Delta} u.$$

We shall here examine the limit of applicability of the above energy density formula. In the homogeneous isotropic medium they are only applicable from the hypocentral distance onward, where  $1/(hr)^2$  is negligible in comparison with  $1/hr$  in which  $h$  means  $2\pi/(\text{wave length})$ . If we assume the wave length to be 10 km.,  $hr$  will be  $1/2\pi$  for  $r=10$  km. And we can apply the formula more or less approximately from the distance of Numadu ( $\Delta=10$  km.) in the North Idu earthquake.

The result of calculation is tabulated in Table XIX, and plotted in Fig. 22 (curve I). The relation  $\left(\frac{1}{\Delta^2}\right)$  due to Mr. Honda is also entered in the same figure for comparison (straight line II). The agreement of the above results are somewhat remarkable, and the writer reported this at the meeting of the Earthquake Research Institute in July 1931. In the discussion at the meeting Prof. Sezawa suspected the result of Dr. Nakano, and in February meeting of the Institute he discussed the variation of amplitude of  $P$ - and  $S$ -waves with distance in a visco-elastic medium,<sup>33)</sup> and showed that "the

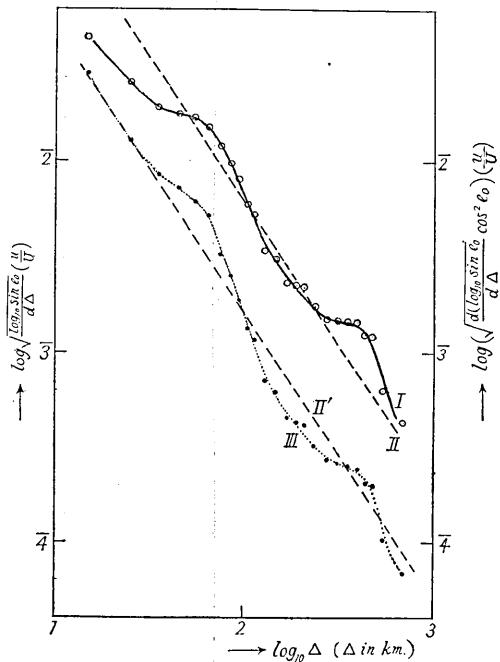


Fig. 22. The variation of amplitude of horizontal motion of  $P$ -wave with epicentral distance. (Hypocentral depth is null.)

33) K. SEZAWA and K. KANAI, *Bull. Earthq. Res. Inst.*, 10 (1932), 299~334.

Table XIX. Calculation of the rate of variation of amplitude of *P*-wave for the North Idu and Itô earthquakes.

$\Delta$	$\cos e$	$10 + \log \sin e$	$\Delta$	$\sqrt{\frac{d(\log_{10} \sin e_0)}{d\Delta}}$	$\frac{u}{U}$	$\log_{10} \sqrt{\Delta} u$	$\log \Delta$	$\log \sqrt{\Delta} u \cos^2 e$
km.			km.	$\times 10^6$ , km.				
0	1.000	—						
10	820	9.75440	15	2820	1.98	2.646	1.176	2.454
20	731	9.83401	25	1653	1.56	2.411	1.398	2.107
30	687	9.86133	35	7283	1.48	2.279	1.544	3.932
40	656	9.87781	45	1246	1.42	2.248	1.653	3.863
50	623	9.89333	55	1234	1.37	2.228	1.740	3.792
60	586	9.90856	65	1164	1.30	2.180	1.813	3.692
70	549	9.92212	75	986	1.23	2.083	1.875	3.538
80	519	9.93185	85	826	1.18	2.014	1.929	3.404
90	496	9.93868	95	706	1.13	1.902	1.978	3.275
100	478	9.94367	105	539	1.11	1.777	2.021	3.127
110	467	9.94657	115	481	1.09	1.720	2.061	3.051
120	458	9.94888	130	315	1.08	1.532	2.114	4.846
140	450	9.95086	150	292	1.07	1.495	2.176	4.795
160	443	9.95256	170	291	1.06	1.366	2.231	4.656
180	439	9.95352	190	216	1.05	1.356	2.270	4.938
200	435	9.95445	210	214	1.04	1.347	2.322	4.621
220	431	9.95538	240	169	1.03	1.241	2.380	4.505
260	426	9.95652	280	149	1.01	1.178	2.447	4.433
300	422	9.95741	320	149	1.00	1.173	2.505	4.420
340	418	9.95830	360	148	99	1.166	2.556	4.404
380	414	9.95918	400	146	99	1.160	2.602	4.390
420	410	9.96003	440	126	98	1.092	2.644	4.315
460	407	9.96067	480	126	99	1.087	2.681	4.304
500	404	9.96131	550	66	96	1.802	2.740	4.013
600	402	9.96174	700	44	96	4.626	2.845	5.825
800	400	9.96212						

amplitude of *S*-wave at a certain distance is more damped than that of *P*-wave at the same distance provided the periods of vibrations of both kinds of waves are the same." and Prof. Sezawa stated that "the abnormal smallness of *P*-wave (as the relation due to Mr. Honda that

the amplitude of  $P$ -wave diminishes with inverse square of distance while that of  $S$ -wave varies inversely with epicentral distance) cannot be ascertained directly from the nature of propagation of waves, but they may be cleared when the mechanism, that the period of  $P$ -wave is small compared with that of  $S$ -wave, will be completely determined." Of course it would be necessary to consider the above effect if the damping due to the viscosity within the crust were very large, but the effect does not seem to be so large from the previous results, so we shall left this, for the moment, untouched.

But we have still to examine the assumption involved in the preceding consideration, that is, the assumption that the energy is emitted uniformly in all directions from the hypocentre. So even if we combine this with the variation of amplitude with azimuth  $\{\sin 2(\varphi + \varepsilon)\}$ , yet it is independent with the colatitude  $\theta$ , that is the angle subtended by the seismic vertical and a seismic ray. But it is very doubtful that there exist such mechanism that give rise such wave which is proportional to  $\sin 2(\varphi + \varepsilon)$  but is independent of  $\theta$ . The writer has already shown that in preceding chapters that the waves due to earthquakes seem to satisfy the equation of wave motion in elastic medium. The investigations in the same line of Mr. Honda<sup>34)</sup> and Mr. M. Takehana<sup>35)</sup> ascertain the proposition. Therefore if this is allowed to be true, the waves dependent on  $\varphi$  can never satisfy the equation of motion independently with  $\theta$ . If we explain the earthquakes by the mechanism of model  $A$  following the suggestion of Prof. Ishimoto, or if we adopt the mechanism of model  $B$ , the waves in any case are dependent on  $\theta$ . But the first mechanism is not immediately applied to the case here concerned (hypocentre is on the surface of Mr. Honda's model of crustal structure), and the discussion of the mechanism of model  $A$  is omitted here, and only the mechanism of model  $B$  will be discussed. Though there are at least two cases in the mechanism of model  $B$  (Prof. Matuzawa's type and Prof. Hasegawa's type), the  $P$ -wave is identical in both cases, and the radial component of motion is proportional to  $\sin^2 \theta \sin 2(\varphi + \varepsilon) = \cos^2 e_0 \sin 2(\varphi + \varepsilon)$  in the above coordinate system (Cf. equation (30) of Chapter II).  $\cos^2 e_0$  is therefore multiplied to the factor already obtained which expresses the variation of surface amplitude with epicentral distance. The result is

34) H. HONDA, *Geophys. Mag.*, 5 (1932), 301~326; 7 (1933), 275~267.

35) M. TAKEHANA, *Kensin Zihô*, 7 (1933), 71~81.

tabulated in 9th column of Table XIX, and plotted in Fig. 22 (curve III). On seeing the diagram we can perceive that better approximation is now obtained to the observed relation (straight line II').

But there remains a question whether the observed  $S$ -wave of these earthquakes may be elucidated or not by the same assumptions of mechanism and crustal structure. Mr. H. Honda said that the amplitudes of  $S$ -waves of these earthquakes were proportional to

$$\frac{1}{\Delta} \cos 2(\varphi + \varepsilon),$$

but there are no bodily waves in the homogeneous isotropic medium that show such a simple relation. And if the above relation is really the case, then fails the writer's explanation in which the actual structure of the crust is taken into consideration. But on examining the actual circumstance we find a fact which is in favour of the writer's explanation, that is the largeness of  $S$ -wave at points where  $2(\varphi + \varepsilon)$  is nearly  $\frac{\pi}{2}$ .

Mr. Honda give in his paper the angle in case of the North Idu earthquake at Tôkyô is  $2(\varphi + \varepsilon) = 92^\circ$ , and that of Yokohama in case of the West Saitama earthquake (which is also explained by the same mechanism by Mr. Honda) is  $2(\varphi + \varepsilon) = 88^\circ$ , but we see in the seismograms of the North Idu earthquake observed at Tokyo indicated in Prof. Imamura's Paper a large and clear  $S$ -phase and Mr. Honda gave as the ratio of amplitudes of  $S$ - and  $P$ -waves due to an after-shock of the earthquake  $S_H/P_H = 5.43$ , while in the seismograms due to an aftershock of the West Saitama earthquake observed at Yokohama which is reproduced in Mr. Honda's paper we find a conspicuous  $S$ -phase. All these earthquakes were explained by Mr. Honda by the mechanism of occurrence due to Dr. Nakano. According to Dr. Nakano's theoretical result the ratio of amplitudes of horizontal motions due to  $S$ - and  $P$ -waves is given by

$$\frac{S_H}{P_H} = \frac{|\vartheta_{a\varphi}|}{|\vartheta_{a\pi}|} = 0.45 \frac{\Delta}{l_1} \cot 2(\varphi + \varepsilon),$$

where  $l_1$  is the wave length of  $P$ -wave. And the ratio  $S_H/P_H$  for Tôkyô ( $\Delta = 99$  km.,  $2(\varphi + \varepsilon) = 92^\circ$ ) in case of North Idu earthquake becomes

$$S_H/P_H = 0.15$$

from the above formula using the value of  $l_1 = 10$  km. deduced by Mr. Honda. The same value for Yokohama ( $\Delta = 76$  km.,  $2(\varphi + \varepsilon) = 88^\circ$ )

in case of the West Saitama earthquake comes out  $1.2/l_1$  ( $l_1$ =wave length in km.), and this may not be much different from the above value. The difference of order of calculated magnitude of  $S_H/P_H$  from the observed one is very hard to be explained by the inaccuracy of determination of  $2(\varphi + \varepsilon)$  or  $l_1$ . But from the writer's explanation by bodily waves due to mechanism of model *B* we may expect tolerably large displacement in *S*-phase even when  $2(\varphi + \varepsilon) = -\frac{\pi}{2}$  in both of mechanisms of Prof. Hasegawa's and Prof. Matuzawa's types (see (86) and (87)).

The writer has proposed in this article an alternative explanation of the interesting relation found and explained by Mr. Honda. It is sufficient to explain the amplitude of *P*-wave by improving unreasonable assumption of homogeneity of earth's crust which is involved in Mr. Honda's explanation. And if the present assumption is permissible we may conclude the damping due to viscosity in the earth's crust is not so effective. On the other hand the writer could not find the same relation in the *S*-phase from the writer's assumption with that deduced by Mr. Honda, but on examining the observed fact closely the writer could find a fact which is unfavourable to Mr. Honda's explanation but easily explained by the writer's alternative hypothesis.

But the writer does not claim the validity of his explanation from the single example, because the later study (which has already been stated in the preceding chapter) showed that the crustal structure here assumed is not free from objection. So some other examples will be examined.

## 2. The West Saitama Earthquake of S. 21, 1931.

After the proposal by Mr. Honda of the hypothesis of continuous variation of amplitude with epicentral distance, Mr. S. I. Kunitomi<sup>36)</sup> discusses in favour of the hypothesis in the study of the West Saitama earthquake, but as he did not examine quantitatively we shall examine it a little in the following. Mr. Kunitomi deduced the variation of amplitude of *P*-wave (resultant of observed horizontal and vertical

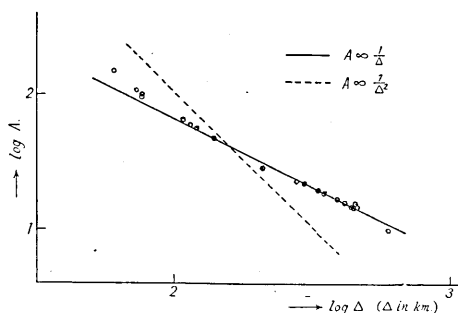


Fig. 23. Variation of amplitude of *P*-wave due to the West Saitama earthquake. (After S. I. Kunitomi.)

36) S. I. KUNITOMI, *Kensin Zihô*, 5 (1932), 223-224.

component) with epicentral distance graphically and of course there may be some arbitrariness in his procedure, but we shall here confine ourselves to the discussion of the values obtained by Mr. Kunitomi which are compiled in  $(\log A - \log \Delta)$  diagram (Fig. 23) which is the same with that of Mr. Honda. We see from the figure a distinct difference from the relation deduced by Mr. Honda already cited. The relation deduced by Mr. Kunitomi is rather near  $\frac{1}{\Delta}$ . Though Mr. Kunitomi's relation was obtained from the resultant of horizontal and vertical motion, while Mr. Honda's result was deduced from the horizontal component only. But the difference cannot be the cause of the above difference  $\frac{1}{\Delta}$  from  $\frac{1}{\Delta^2}$ , on the contrary the use of horizontal component will decrease the rate of variation with epicentral distance.

### 3. *The Tango Earthquake of Mar. 7, 1927.*

Mr. Honda<sup>37)</sup> pointed out that the above earthquake was also originated by the same mechanism as those of North Idu, Itô and West Saitama earthquakes. As there is a valuable report of this earthquake by Mr. S. I. Kunitomi,<sup>38)</sup> let us borrow the necessary data from his paper and examine the point in question.  $\Delta$  and  $A$  in Table XX is directly extracted from his paper and  $\varphi + 29^\circ$  ( $\varphi =$  azimuth) is the bearing of the station from a nodal line which is measured on a map showing the "pull-push" distribution in Mr. Kunitomi's paper. Therefore no high accuracy can be claimed, but the general trend will not be affected by it. Following Mr. Honda, the variation of amplitude  $A$  (horizontal component) with azimuthal angle was cancelled by deviding  $A$  by  $\sin 2(\varphi + 29^\circ)$  and the result ( $A_n$ ) is indicated in Table XX and Fig. 24. On seeing the diagram we are bewildered at the heavy scattering of the points, but the mean value

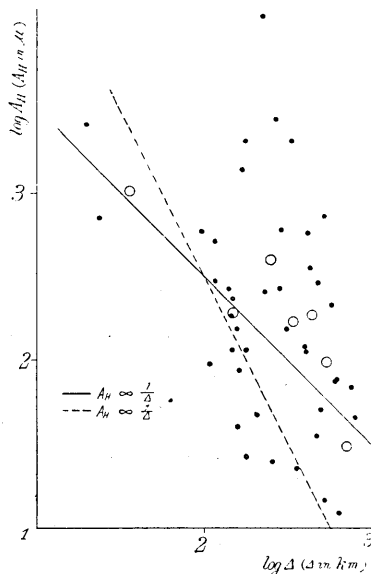


Fig. 24. Variation of horizontal component of  $P$ -wave due to the the Tango earthquake.

37) H. HONDA, *Geophys. Mag.*, 5 (1932), 69~88.

38) S. I. KUNITOMI, *Geophys. Mag.*, 2, (1929), 65~89.

Table XX. Variation of magnitude of initial motion of the Tango earthquake.

Station	$\Delta$ in km.	$\varphi + 29^\circ$	$A$ in $\mu$	$\log \frac{A\mu}{\sin 2(\varphi + \varepsilon)}$	$\log \Delta$
Miyadu	20	169°	960	3.409	1.301
Kyōto	97	171	180	2.765	1.987
Hikone	117	143	283	2.469	2.068
Hukui	116	93	140	2.706	2.064
Kanazawa	178	87	12	2.060	2.250
Gihu	158	129	151	2.189	2.199
Nagoya	176	137	2040	3.311	2.246
Tu	170	156	1020	2.138	2.230
Yagi	144	179	4	2.059	2.167
Hamamatu		141	260	2.425	2.149
Toyama	209	101	18	1.682	2.320
Husiki	223	87	1180	4.053	2.348
Nagano	306	98	43	2.193	2.486
Takada	332	89	71	3.309	2.521
Numadu	352	128	22	1.356	2.547
Kumagaya	399	110	77	2.078	2.601
Tōkyō	431	116	230	2.551	2.634
Kakioka	472	110	23	1.554	2.674
Tyōsi	530	117	585	2.859	2.724
Sendai	598	93	8	1.884	2.777
Akita	640	73	7	1.098	2.806
Morioka	765	78	28	1.833	2.884
Kōbe	108	202	61	1.978	2.033
Wakayama	160	205	31	1.607	2.204
Sumoto	145	214	168	2.258	2.161
Sionomisaki	255	193	11	1.399	2.407
Tokusima	179	223	27	1.432	2.253
Kōti	267	240	289	3.437	2.427
Sakai	163	298	74	1.940	2.212
Hamada	280	283	118	2.430	2.447
Hirosima	231	299	9	2.411	2.364
Ōita	411	258	46	2.054	2.614
Miyazaki	527	249	10	1.174	2.722
Kumamoto	505	262	14	1.706	2.703
Kagosima	612	253	43	1.885	2.787
Nagasaki	570	266	30	2.333	2.756
Hukuoka	480	271	10	2.457	2.681
Simonoseki	416	272	40	2.758	2.619
Zinsen	800	316	46	1.663	2.903
Okayama	149	253	131	2.369	2.173
Matuyama	285	255	3	2.778	2.455
Toyooka	24	268	51	2.854	1.380

by every 100km. interval (○ in Fig. 24) does not show such steep decrease of amplitude as  $\frac{1}{\Delta^2}$  (broken line in Fig. 24) and nearly proportional to  $\frac{1}{\Delta}$  (shown by a full line in the diagram). It may be added that the sudden decrease of amplitude at about  $\log_{10}\Delta=2.2$  (or  $\Delta=160$  km.) may be interpreted, if real, by the sudden decrease of energy density near the place where  $P_n$ -wave makes its first appearance owing to discontinuity surface in the crust. If the distance ( $\Delta=190$  km.) is the radius of the critical circle then the hypocentre of the earthquake will be deeper than 20 km. in the single-layer model by Dr. Wadati and others. Anyhow, the above difference of the rate of decrease of amplitude with  $\Delta$  from that obtained by Mr. Honda is therefore to be examined whether it is due to finite focal depth or not.

Fortunately Dr. Wadati has calculated adopting the velocity distribution given by Mr. Honda, the time distance curves and cosines of emergency angle for various hypocentral depths. We can therefore calculate the amplitude in the same way as for

the North Idu and Itô earthquakes. The variation of amplitude of horizontal motion with epicentral distance due to variation of energy density and surface reflexion, thus calculated (Table XXI), is denoted in Fig. 25, curve I, while the corrected value for the variation with  $\theta\left(=\frac{\pi}{2}-e_n\right)$  due to the mechanism of model B by multiplying  $\cos^2 e_n$  is denoted by the curve II in Fig. 25. These two curves denote the variation nearly proportional to  $\frac{1}{\Delta^2}$  from the distance  $\Delta=40$  km. ( $\log_{10}\Delta=1.6$ ) onward. Comparing these curves with the observed values in Fig. 24, we cannot find no close correlation. The variation of hypocentral depth will have little effect on this conclusion, so far as the earthquakes of shallow origin is concerned.

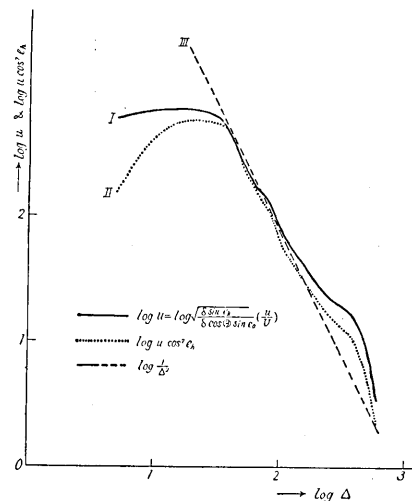


Fig. 25. Variation of amplitude of horizontal motion of  $P$ -wave with epicentral distance. (Hypocentral depth = 20 km.)

#### 4. Concluding remark of Chapter VII.

Table XXI. Variation of amplitude of horizontal component of  
*P*-wave on the earth's surface for the earthquake with  
 hypocentral depth 20 km. (Calculated.)

$\Delta$ km.	$\cos e_0$	$\cos e_h$	$\Delta$	$\log \frac{\delta(\sin e_h)}{\delta(\cos \theta) \sin e_0}$	$\log u$	$\log A_H = \log u \cos^2 e_h$	$\log \Delta$
0	0.000	0.0000	5	6.325	2.781	2.189	0.699
10	0.281	0.5585	15	5.888	2.852	2.554	1.176
20	0.423	0.8407	25	5.630	2.825	2.741	1.396
30	0.476	0.9460	35	5.406	2.748	2.739	1.544
40	0.497	0.9878	45	5.002	2.541	2.525	1.653
50	0.488	0.9699	55	4.624	2.346	2.314	1.740
60	0.481	0.9560	65	4.406	2.233	2.187	1.813
70	0.474	0.9421	75	4.267	2.158	2.100	1.875
80	0.467	0.9282	85	4.128	2.082	2.012	1.929
90	0.461	0.9192	95	3.890	1.957	1.876	1.978
100	0.455	0.9043	110	3.638	1.827	1.733	2.041
120	0.448	0.8904	130	3.449	1.726	1.619	2.114
140	0.442	0.8785	150	3.285	1.641	1.524	2.176
160	0.438	0.8705	170	3.155	1.573	1.449	2.230
180	0.434	0.8620	190	3.029	1.504	1.372	2.279
200	0.431	0.8566	210	2.992	1.443	1.306	2.322
220	0.428	0.8506	230	2.828	1.398	1.255	2.362
240	0.426	0.8467	250	2.758	1.361	1.214	2.398
260	0.424	0.8427	270	2.696	1.330	1.178	2.431
280	0.421	0.8367	290	2.655	1.307	1.150	2.462
300	0.419	0.8328	310	2.916	1.286	1.125	2.491
320	0.417	0.8288	330	2.584	1.267	1.102	2.519
340	0.415	0.8248	350	2.552	1.248	1.080	2.544
360	0.414	0.8228	370	2.521	1.231	1.060	2.568
380	0.412	0.8188	390	2.464	1.200	1.024	2.591
400	0.410	0.8149	410	2.397	1.164	0.984	2.613
420	0.408	0.8109	430	2.304	1.115	0.931	2.633
440	0.407	0.8089	450	2.169	1.045	0.858	2.653
460	0.405	0.8049	470	2.137	1.028	0.838	2.672
480	0.404	0.8029	490	2.053	0.976	0.784	2.690
500	0.403	0.8010	520	1.760	0.838	0.644	2.716
540	0.402	0.7690	600	1.204	0.559	0.363	2.778
660	0.401	0.7970					

From the above three examples we have seen that the amplitudes of seismic waves are closely connected with the structure of earth's crust, and conversely we can discuss the crustal structure effectively from the observation of the magnitudes of first motions of seismic waves. It is therefore an interesting and important matter to ascertain these problems from the examination of these points.

The amplitude of seismic waves due to the North Idu and Ito earthquakes seemed to have been well explained by the mechanism of model *B* on the assumption of crustal structure due to Mr. Honda. But on examining the West Saitama and Tango earthquakes for the verification we cannot find the same relation expressing the variation of amplitude with epicentral distance as that which was deduced from the North Idu and Ito earthquakes by Mr. Honda. Though the relation here obtained may be doubtful owing to the methodological and observational inaccuracies, we have still better to call attention for the necessity of confirmation of this important problem, because we have already seen some ambiguity in the hypothesis of crustal structure assumed in this chapter. The writer's true object is to point out these necessities and a method of solution for the future occasions.

### Chapter VIII. Concluding Remarks.

For the quantitative elucidation of seismic waves the writer discusses in this paper two main factors determining the first motions of seismic waves, namely the mechanism of occurrence of earthquake and the structure of the earth's crust. Though there are a number of investigations either in the theoretical side of the waves in and on elastic body, or in practical side, of the mechanism of earthquake occurrence by the observation of "pull-push" distribution of *P*-wave, these investigations have stood side by side independently, and only one investigation has been carried out quantitatively combining these two sides, but neglect of the important effect due to the crustal structure has been a very serious matter. Though the strict and rigorous theory on waves in heterogeneous medium applicable to the actual case is still absent, the writer introduced a simple method to calculate the effect of crustal structure on the amplitude of seismic body waves. They are practically the same as the energy density method due to K. Zöppritz and E. Wiechert.

In combining the method with the solutions which have been deduced generally in a simple and formal way, the writer examined a

few cases of interest quantitatively. From the present study of the *P*- and *S*-waves of these examples we could see the existence of both mechanisms of model *A* and model *B*, in answer to the questions proposed by Prof. Ishimoto that "by which of the mechanisms of model *A* and model *B* the earthquakes are originated." On obtaining the expression of *P*- and *S*-waves the writer could infer the magnitudes and directions of earthquake generating forces and energy carried away by seismic waves from the hypocentre.

Necessity of higher accuracy in the seismometrical observations is keenly felt for such a purpose. As to the mechanism of earthquake occurrence there is a question whether it is confined to the above mechanisms or not. Moreover we have also to examine the magnitude of vertical angle of the nodal cone in the mechanism of model *A*, because it was proved to be arbitrary from the theoretical point of view. The same is true for the angle subtended by two nodal planes in the mechanism of model *B*, as will be easily understood by superposing the waves due to two pairs of doublet without moment with different signs and magnitudes which are acting at right angles to each other. We have also seen the necessity of examining to existence of the *S*-waves of second kind which may exist independently from the mechanisms that give rise *P*-waves.

Thus there still remains some problems in the mechanisms of earthquake occurrence to be cleared with the improved observations. But from the applications of the knowledge which has been obtained above, the writer has shown the possibility to determine interesting informations concerning the hypocentre, as its position and dimension and the phenomena occurring there as well as the structure of the earth's crust. The possibility of these problems and methods to reach the objects were pointed out in near earthquakes. The solution of internal structure of the earth is promised to the observations of distant earthquakes.

In conclusion the writer wish to express his sincere thanks and appreciation to Prof. M. Ishimoto for his interest and encouragement throughout the course of this study. His cordial thanks are also due to Professor T. Okada for the kindness to accomodate the writer with valuable data. He is also very much obliged to all the persons from whose papers he could obtain valuable data used in this paper.

---

## 43. 地震波の傳播 (第 2 報)

## 發震機巧, 地殻構造と地震波の振幅に就て (續き)

地震學教室 河 角 廣

第 IV 章に於けると全く同様な方法を用ひて第 V 章に昭和 4 年 6 月 2 日伊勢灣口に起つた深發地震を定量的に調査した。此の地震に關しては始め鷺坂氏は B-型の地震であるとせられたに對し石本博士は P 波初動「押し, 引き」分布に關する限り A-型の機巧にて極めてよく説明出来る事を指摘されて。其の何れであるか問題視されて居たが本調査により B-型機巧の方が簡単に P, S, 兩波の初動方向, 振幅等を説明出来る事が明になつた。然し乍ら石本博士による A-型の機巧にて P-波の説明には充分であり, S 波初動も此の外に第 2 種の S-波を附加すれば説明出来ない事ではなく, 前者との間の相違は僅である。

次に此の地震が B-型機巧によつて起されたものと見ると, 初動分布から震源の位置は  $\varphi = 34^{\circ}30' N$ ,  $\lambda = 136^{\circ}54' E$ , 深さ約 300 軒と定まつた。P-波押波の振幅最大の震波線は震原に於て垂直から北  $80^{\circ}$  西の方向に約  $33^{\circ}$  傾いた方向に出た事になり, 此れは略大阪の近くに出た事になるが不幸にして此の地震は大阪及び神戸にては十分観測出来なかつた。然し乍ら若し観測出来たら此等の所に於ては所謂初期微動なしの地震を観測した事であらう。京都洲本, 和歌浦, 日方等に於て観測された P-波の振幅の大きい事は此れを裏書きして居る。此れを以つて見れば大森博士の調査せられた明治 40 年 2 月 1 日の初期微動なしの地震は遠州沖に全く上の地震と同様な機巧によつて起されたものであらうと考へられる。

S-波の観測から此の地震は松澤先生の斷層地震型によつて起されたものでなく, 長谷川助教の型に近いもので起された事が知られたが, 更に P 波, S 波の振幅の比を精査するに及んで長谷川助教の型から豫期されるものより, S 波が小さかつた事が知られたが, 此れを地殻の粘性による減衰によつて説明するは困難である様に見へる。次に此の地震に於て波として震原から運ばれる勢力は毎秒  $3.7 \times 10^{19}$  エルグと出, 其の總量は約  $10^{21}$  エルグの程度のものであつたと考へられる。

次に第 VI 章及び第 VII 章に於ては淺發地震にも前 2 章と同様な彈性波動論的取扱が, 地殻構造を考慮に入れば應用出来る事を示すと共に逆に此の方法を用ひて地殻構造, 震原の位置等を推定出来る事を示した。即第 VI 章には昭和 3 年 7 月 27 日の相模中部の地震の初動分布に見られる特異性が A-型機巧と地殻構造に由來する事を指摘し, 此の説明には震央距離 200 軒以下の所に於て射出角が不連続的に變化する所があるとなしければならぬことを示し, 地表近くに不連続面が存在するとの假設が有利である事を示した。第 VII 章には淺發地震の振幅の定量的吟味をなし, 北伊豆及伊東地震に於て本多氏の見出された P-波振幅に關する關係が中野博士の理論によらなくても B 型の發震機巧と本多氏の地殻構造とから深發地震に用ひたと全く同様な方法で説明出来る事を知つたが, 本多氏による地殻構造は第 VII 章に於て見出された事實を説明する事が出来なかつたから更に進んで西埼玉地震及び丹後地震に就て同様な調査をして見たが本多氏の見出された様な P-波の振幅が震央距離の自乗に逆比例すると云ふ關係は見出せなかつたから此の方面から地殻構造を決定するには更に多數の地震を調査する必要がある事を示した。

地震の發震機巧が A 型であるか, B 型であるかの問題について始めた研究も此處に兩方ともに

存在すると云ふ結論に到達した。筆者について本多氏も深発地震の *P*-波に關する定量的の研究をされ *B*-型の機巧で起された地震を確められ、其の後竹花氏、筆者及び吉山氏、本多氏と鷺坂氏、竹花氏等の研究により *B*-型の地震も多く見出された。

一方石本博士、筆者及び水上氏の研究から *A*-型の機巧でなければ説明出来ない例も見出された。筆者は地震の發震機巧を知る爲に彈性波動論的の解析的方法を考へ實際の地殻構造をも考慮して地震波の振幅を論じ發震力、地震波勢力の問題をも考へたが此等の點を論ずるには地震計測の方法を一層精密にする必要がある事を痛感する。

更に發震機巧にしても上に見た様な機巧だけに限るかは問題であるが節圓錐の表はれる場合にも其の圓錐の頂角の大きさは彈性論的には任意であり得る事を知つたし、節平面の表はれる場合にも其等節平面間の角度は直角に限らず任意であり得る事も能率なしの二重力の大きさも符號も異なるものを 2 組を互に直角の方向に重ね合せる事により簡單に知る事が出来るから今後は此の點をも吟味しなければならぬ。以上の様に發震機巧にも觀測の整備に伴ひ考察の餘地が残つて居るが、上に得た知識の應用により逆に地震波の振幅から震原の位置、地殻構造を知る事が可能である事を近地地震に就て示し、更に遠地地震に於てこれを論ずれば地球内部の構造が論ぜられる譯であるが此れは第 3 報に譲る事にする。

數年に亙る此等の研究に斷へざる理解と御鞭撻を賜つた地震研究所長石本博士に先づ深甚の感謝の意を表し、又此等の研究の材料を拜借させて頂いた棚橋氏、鷺坂氏、牟田氏、本多氏並に國富氏に厚く謝意を表し、御便宜を與へられた氣象臺長岡田博士に厚く御禮申上げる。尙此の論文に於て諸氏の論文に言及した失禮は深く御詫び申上げると共に筆者の妄言は充分に御叱正の程を御願する。